Technology of Japan and grants from the Foundation for the Development of the Community (Tochigi, Japan).

Disclosures

J.I. is supported in part by a grant of Mitsubishi Pharma Research Foundation. The remaining authors report no conflicts.

References

1. Verdecchia P, Schillaci G, Borgioni C, Ciucci A, Gattobigio R, Zampi I, Porcellati C. Prognostic value of a new electrocardiographic method for diagnosis of left ventricular hypertrophy in essential hypertension. *J Am Coll Cardiol*. 1998;31:383–390.
2. Levy D, Garrison RJ, Savage DD, Kannel WB, Castelli WP. Prognostic implications of echocardiographically determined left ventricular mass in the Framingham heart study. *N Engl J Med*. 1990;322:1561–1566.
3. Sokolow M, Lyon T. The ventricular complex in left ventricular hypertrophy as obtained by unipolar precordial and limb leasds. *Am Heart J*. 1949;37:161–186.
4. Molloy T, Okin P, Devereux R, Kligfield P. Electrocardiographic detection of left ventricular hypertrophy by the simple QRS voltage-duration product. *J Am Coll Cardiol*. 1992;20:1180–1186.
5. Okin PM, Roman MJ, Devereux RB, Kligfield P. Electrocardiographic identification of increased left ventricular mass by simple voltage-duration products. *J Am Coll Cardiol*. 1995;25:417–423.
6. Okin PM, Devereux RB, Jern S, Julius S, Kjeldsen SE, Dahlof B. Relation of echocardiographic left ventricular mass and hypertrophy to persistent electrocardiographic left ventricular hypertropy in hypertensive patients: the LIFE Study. *Am J Hypertens*. 2001;14:775–782.
7. Okin PM, Devereux RB, Jern S, Kjeldsen SE, Julius S, Nieminen MS, Snapinn S, Harris KE, Aurup P, Edelman JM, Wedel H, Lindholm LH, Dahlof B, for the LIFE Study Investigators. Regression of electrocardiographic left ventricular hypertrophy during antihypertensive treatment and the prediction of major cardiovascular events. *JAMA*. 2004;292:2343–2349.
8. Ishikawa S, Kazuomi K, Kayaba K, Gotoh T, Nago N, Nakamura Y, Tsutsumi A, Kajii E, Jichi Medical School (JMS) Cohort Study Group. Linear relationship between blood pressure and stroke: the Jichi Medical School Cohort Study. *J Clin Hypertens (Greenwich)*. 2007;9:677–683.
9. Palmieri V, Bella JN, Arnett DK, Liu JE, Oberman A, Schuck M-Y, Kitzman DW, Hopkins PN, Morgan D, Rao DC, Devereux RB. Effect of type 2 diabetes mellitus on left ventricular geometry and systolic function in hypertensive subjects: Hypertension Genetic Epidemiology Network (HyperGEN) study. *Circulation*. 2001;103:102–107.
10. Bella JN, Devereux RB, Roman MJ, Palmieri V, Liu JE, Paranicas M, Welty TK, Lee ET, Fabsitz RR, Howard BV. Separate and joint effects of systemic hypertension and diabetes mellitus on left ventricular structure and function in American Indians (the Strong Heart Study). *Am J Cardiol*. 2001;87:1260–1265.
11. Okin PM, Devereux RB, Gerdts E, Snapinn SM, Harris KE, Jern S, Kjeldsen SE, Julius S, Edelman JM, Lindholm LH, Dahlof B, for the LIFE Study Investigators. Impact of diabetes mellitus on regression of electrocardiographic left ventricular hypertrophy and the prediction of outcome during antihypertensive therapy: the Losartan Intervention for Endpoint (LIFE) reduction in hypertension study. *Circulation*. 2006;113:1588–1596.
12. Ishikawa S, Gotoh T, Nago N, Kayaba K. The Jichi Medical School (JMS) cohort study: design, baseline data and standardized mortality ratios. *J Epidemiol*. 2002;12:408–417.
13. Ishikawa S, Kayaba K, Gotoh T, Nago N, Nakamura Y, Tsutsumi A, Kajii E. Incidence of total stroke, stroke subtypes, and myocardial infarction in the Japanese population: the JMS Cohort Study. *J Epidemiol*. 2008;18:144–150.
14. Sekine M, Gotoh E, Ochiai H, Umezu M, Ishii M. Office blood pressure in patients with essential hypertension. *Ther Res*. 1997;18:122.
15. The world health organization MONICA project (monitoring trends and determinants in cardiovascular disease): a major international collaboration. Who MONICA project principal investigators. *J Clin Epidemiol*. 1988;41:105–114.
16. Pencina MJ, D'Agostino RB. Overall c as a measure of discrimination in survival analysis: model specific population value and confidence interval estimation. *Stat Med*. 2004;23:2109–2123.
17. Okin PM, Devereux RB, Jern S, Kjeldsen SE, Julius S, Dahlof B. Baseline characteristics in relation to electrocardiographic left ventricular hypertrophy in hypertensive patients: the Losartan Intervention for Endpoint reduction (LIFE) in hypertension study. *Hypertension*. 2000;36:766–773.
18. Shirai T, Kasao M, Nozaki M, Nitta S. Evaluation of hypertensive cardiac abnormalities using the Cornell product. *Circ J*. 2007;71:731–735.
19. Eguchi K, Kario K, Hoshide S, Ishikawa J, Morinari M, Shimada K. Type 2 diabetes is associated with left ventricular concentric remodeling in hypertensive patients. *Am J Hypertens*. 2005;18:23–29.
20. Eguchi K, Ishikawa J, Hoshide S, Ishikawa S, Pickering TG, Schwartz JE, Homma S, Shimada K, Kario K. Differential impact of left ventricular mass and relative wall thickness on cardiovascular prognosis in diabetic and nondiabetic hypertensive subjects. *Am Heart J*. 2007;154:79.e9–e15.
21. Marwick TH. Diabetic heart disease. *Heart*. 2006;92:296–300.
22. Okin P, Wright J, Nieminen MS, Jern S, Taylor A, Phillips R, Papademetriou V, Clark L, Ofili E, Randall O, Oikarinen L, Viitasalo M, Toivonen L, Julius S, Dahlöf B, Devereux R. Ethnic differences in electrocardiographic criteria for left ventricular hypertrophy: the LIFE Study. *Am J Hypertens*. 2002;15:663–671.
23. Sundström J, Lind L, Arnlov J, Zethelius B, Andren B, Lithell HO. Echocardiographic and electrocardiographic diagnoses of left ventricular hypertrophy predict mortality independently of each other in a population of elderly men. *Circulation*. 2001;103:2346–2351.

Biochemical and Biophysical Research Communications 379 (2009) 249–254

Contents lists available at ScienceDirect

Biochemical and Biophysical Research Communications

journal homepage: www.elsevier.com/locate/ybbrc

Skp2 promotes adipocyte differentiation via a $p27^{Kip1}$-independent mechanism in primary mouse embryonic fibroblasts

Mitsuru Okada [a,1], Tamon Sakai [a,1], Takehiro Nakamura [a], Mimi Tamamori-Adachi [b], Shigetaka Kitajima [b], Yasushi Matsuki [c], Eijiro Watanabe [c], Ryuji Hiramatsu [c], Hiroshi Sakaue [a,d,*], Masato Kasuga [a,e]

[a] Division of Diabetes, Metabolism, and Endocrinology, Department of Internal Medicine, Kobe University Graduate School of Medicine, Kobe 650-0017, Japan
[b] Department of Biochemical Genetics, Medical Research Institute, Tokyo Medical and Dental University, Tokyo 113-8510, Japan
[c] Pharmacology Research Laboratories, Dainippon Sumitomo Pharma Co. Ltd., Takarazuka 665-0051, Japan
[d] Department of Pharmacology, Kinki University School of Medicine, Osakasayama 589-8511, Japan
[e] Research Institute, International Medical Center of Japan, Tokyo 162-8655, Japan

ARTICLE INFO

Article history:
Received 27 November 2008
Available online 25 December 2008

Keywords:
$p27^{Kip1}$
Skp2
PPARγ
Cell cycle
Adipogenesis
Adipocyte differentiation

ABSTRACT

Skp2, the substrate-binding subunit of an SCF ubiquitin ligase complex, is a key regulator of cell cycle progression that targets substrates for degradation by the 26S proteasome. We have now shown that ablation of *Skp2* in primary mouse embryonic fibroblasts (MEFs) results both in impairment of adipocyte differentiation and in the accumulation of the cyclin-dependent kinase inhibitor $p27^{Kip1}$, a principal target of the SCF^{Skp2} complex. Genetic ablation of $p27^{Kip1}$ in MEFs promoted both lipid accumulation and adipocyte-specific gene expression. However, depletion of $p27^{Kip1}$ by adenovirus-mediated RNA interference failed to correct the impairment of adipocyte differentiation in $Skp2^{-/-}$ MEFs. In contrast, troglitazone, a high-affinity ligand for peroxisome proliferator-activated receptor γ (PPARγ), largely restored lipid accumulation and PPARγ gene expression in $Skp2^{-/-}$ MEFs. Our data suggest that Skp2 plays an essential role in adipogenesis in MEFs in a manner that is at least in part independent of regulation of $p27^{Kip1}$ expression.

Introduction

The worldwide epidemic of obesity is a serious threat to public health, in part because the increase in the mass of white adipose tissue (WAT) in obese individuals increases the risk for development of type 2 diabetes mellitus and cardiovascular disease. The expansion of WAT during the development of obesity can occur through an increase in cell number (adipocyte hyperplasia) or in cell size (adipocyte hypertrophy) [1,2]. The number of adipocytes is thought to increase as a result of the proliferation of preadipocytes and their subsequent differentiation into mature adipocytes [3,4]. The proliferation of preadipocytes is regulated at each phase of the cell cycle by the activation and deactivation of various proteins including cyclins, cyclin-dependent kinases (CDKs), and CDK inhibitors (CKIs) [5,6]. CKIs include two families of proteins, the Cip (Kip) family and Ink4 family, and are central players in the exit of cells from the cell cycle [7]. Genetic ablation of $p27^{Kip1}$ or $p21^{Cip1}$ in mice leads to adipocyte hyperplasia as a result of increased proliferation or recruitment of preadipocytes [8], suggesting that these CKIs are important in regulation of adipocyte number. The SCF (Skp1-Cullin–F-box protein) ubiquitin ligase (E3) complex targets CKIs for degradation by the 26S proteasome and thereby regulates cell cycle progression [9]. Skp2, the substrate-binding subunit of the SCF^{Skp2} complex, contributes to the degradation of $p27^{Kip1}$, an inhibitor of CDK2 and CDK1 activities that promote entry into S phase and mitosis, respectively. We have recently shown that the increase in adipocyte number that accompanies obesity is associated with up-regulation of Skp2 expression in WAT of mice [10]. Furthermore, ablation of *Skp2* resulted both in inhibition of the increase in adipocyte number and in improvement of obesity-related insulin resistance in obesity-prone mice [10]. However, the precise contribution of Skp2 to adipocyte differentiation has remained unclear. We now show that Skp2 plays an essential role in the differentiation of primary mouse embryonic fibroblasts (MEFs) into adipocytes, and we present evidence that this action of Skp2 occurs independently of the control of cell cycle progression and $p27^{Kip1}$ degradation.

Materials and methods

Antibodies, reagents, and cells. Antibodies to Erk1/2, to $p27^{Kip1}$, and to Skp2 were obtained from Cell Signaling Technologies

* Corresponding author. Address: Department of Pharmacology, Kinki University School of Medicine, School of Medicine, 377-2 Onohigashi, Osakasayama 589-8511, Japan. Fax: +81 072 366 1820.
E-mail address: hsakaue@med.kindai.ac.jp (H. Sakaue).
[1] These authors contributed equally to this work.

0006-291X/$ - see front matter © 2008 Elsevier Inc. All rights reserved.
doi:10.1016/j.bbrc.2008.12.069

(Beverly, MA), Santa Cruz Biotechnology (Santa Cruz, CA), and Invitrogen Corporation (Carlsbad, CA), respectively. Troglitazone was kindly provided by Daiichi Sankyo Co. Ltd. (Tokyo, Japan). 3T3-L1 cells were obtained from American Type Culture Collection (Manassas, VA).

Animals. Male C57BL/6 mice were obtained from CLEA Japan. Mice lacking Skp2 [11] or $p27^{Kip1}$ [12] were kindly provided by K. Nakayama (Tohoku University, Japan) and K.I. Nakayama (Kyushu University, Japan). Parental $Skp2^{+/-}$mice used to generate $Skp2^{+/+}$, $Skp2^{+/-}$, and $Skp2^{-/-}$ mice as well as parental $p27^{+/-}$ mice used to generate $p27^{+/+}$ and $p27^{-/-}$ mice were derived by backcrossing the C57BL6/129SV mutants to the C57BL/6 background for seven or eight generations [10]. Mouse experiments were performed according to the guidelines of the animal ethics committee of Kobe University Graduate School of Medicine.

Cell culture and staining. MEFs ($p27^{+/+}$, $p27^{-/-}$, $Skp2^{+/+}$, $Skp2^{+/-}$, or $Skp2^{-/-}$) were derived from littermates of the corresponding genotype at embryonic day 13.5 and were cultured as described previously [13]. The differentiation of MEFs into adipocytes was induced by incubation of confluent cells for 6 days with insulin (5 μg/ml), 1 μM dexamethasone, and 0.5 mM isobutylmethylxanthine in Eagle's minimum essential medium supplemented with 10% fetal bovine serum. The cells were then returned to basal medium, which was replenished every other day. The differentiation of 3T3-L1 preadipocytes into adipocytes was induced as previously described [14]. Cells were stained with oil red O as described [15].

Retroviral and adenoviral vectors. 3T3-L1 cells stably expressing $p27^{Kip1}$ were generated by infection with a retroviral vector encoding human $p27^{Kip1}$ as described previously [13]. An adenoviral vector encoding a small interfering RNA (siRNA) specific for $p27^{Kip1}$ mRNA was also generated as described previously [16]. An adenoviral vector encoding β-galactosidase was kindly provided by I. Saito (University of Tokyo, Japan). For adenovirus-mediated gene transfer, primary MEFs cultured to 30–50% confluence were infected for 6 h with adenoviral vectors at a multiplicity of infection of 10 plaque-forming units per cell on the day after their isolation from embryos. The cells were then transferred to a new culture dish at a density of 1.2×10^5 cells/cm^2 and cultured for up to 24 h to ~100% confluence. After culture for an additional 3 days, differentiation of the MEFs into adipocytes was induced as described above.

Flow cytometry and cell counting. At various times after the induction of adipocyte differentiation as described above, 3T3-L1 cells and MEFs were washed with phosphate-buffered saline, isolated by exposure to trypsin, fixed with 70% ethanol, and incubated for 30 min at 37 °C with RNase A (1 mg/ml). After staining with propidium iodide (20 μg/ml), the cells were analyzed for DNA content by flow cytometry. The number of cells was counted with the use of a counting chamber (Erma).

Immunoblot and real-time quantitative RT-PCR analyses. Immunoblot analysis was performed as described previously [15]. Reverse transcription and real-time quantitative polymerase chain reaction (qRT-PCR) analysis was performed as described [17] with a sequence detector (model 7900, Applied Biosystems). The PCR primers were described in Supplementary materials and methods.

Results and discussion

Effect of overexpression of $p27^{Kip1}$ on adipocyte differentiation in 3T3-L1 cells

3T3-L1 preadipocytes are a well-characterized model for studying adipocyte differentiation [18]. On exposure to insulin, dexamethasone, and IBMX, these cells undergo one or two rounds of cell division, a process known as mitotic clonal expansion [19], before they begin to accumulate lipid and to express adipocyte marker genes. Indeed, the number of 3T3-L1 cells had increased by a factor of ~2.3 or ~3.4 at 48 or 96 h, respectively, after the onset of induction of differentiation (Fig. S1A). During this period of mitotic clonal expansion, the abundance of $p27^{Kip1}$ initially decreased and that of Skp2 increased (Fig. S1B), consistent with previous observations [20–22].

To determine whether this down-regulation of $p27^{Kip1}$ expression is required for adipocyte differentiation, we examined the effect of overexpression of $p27^{Kip1}$ with the use of a retroviral vector on the induction of mitotic clonal expansion, lipid accumulation, and the expression of adipocyte marker genes in 3T3-L1 cells. At 18 h after the onset of exposure to inducers of differentiation, the amount of $p27^{Kip1}$ in the $p27^{Kip1}$-overexpressing cells had decreased, as it had in cells infected with the corresponding empty vector, but the abundance of $p27^{Kip1}$ in the former cells was markedly greater than that in the latter (Fig. 1A). Overexpression of $p27^{Kip1}$ substantially inhibited both lipid accumulation (Fig. 1B) and the increases in the abundance of PPARγ1, PPARγ2, 442/aP2, and GLUT4 mRNAs (Fig. 1C) that are normally apparent 8 days after the onset of exposure of 3T3-L1 cells to the inducers of differentiation. Furthermore, the increase in the number of $p27^{Kip1}$-overexpressing 3T3-L1 cells at 48 h after the onset of differentiation induction was markedly smaller than that for cells infected with the empty vector (Fig. 1D). We next examined cell cycle progression in $p27^{Kip1}$-overexpressing 3T3-L1 cells by flow cytometric analysis. Whereas ~56% of control cells had entered S or G_2-M phases after exposure to inducers of differentiation for 18 h, only ~26% of $p27^{Kip1}$-overexpressing cells had done so (Fig. 1E). These results indicated that mitotic clonal expansion of 3T3-L1 cells was inhibited by overexpression of $p27^{Kip1}$, and they suggested that $p27^{Kip1}$ may regulate adipocyte differentiation by controlling cell proliferation during mitotic clonal expansion in these cells.

Impaired adipogenesis in MEFs isolated from $Skp2^{-/-}$ mice

The Skp2-dependent degradation of $p27^{Kip1}$ directly regulates cell division during mitotic clonal expansion in 3T3-L1 preadipocytes [22,23]. To determine whether Skp2 is required for adipocyte differentiation, we isolated MEFs from $Skp2^{+/+}$, $Skp2^{+/-}$ and $Skp2^{-/-}$ littermates at embryonic day 13.5. Immunoblot analysis revealed that the amount of $p27^{Kip1}$ is markedly increased in $Skp2^{-/-}$ MEFs compared with that in $Skp2^{+/+}$ or $Skp2^{+/-}$ MEFs (Fig. S2A). The amount of $p27^{Kip1}$ mRNA was slightly decreased in $Skp2^{-/-}$ MEFs relative to that in $Skp2^{+/+}$ cells, but the difference was not statistically significant (Fig. S2B). Whereas 30–40% of $Skp2^{+/+}$ or $Skp2^{+/-}$ MEFs exhibited cytoplasmic lipid accumulation at 10 days after the onset of differentiation induction, <10% of $Skp2^{-/-}$ MEFs did so (Fig. 2A). Furthermore, the amounts of mRNAs for the adipocyte markers PPARγ1, PPARγ2, 442/aP2, and GLUT4 were significantly reduced in $Skp2^{-/-}$ MEFs compared with those in $Skp2^{+/+}$ MEFs at this time (Fig. 2B). The abundance of PPARγ1, PPARγ2, 442/aP2, and GLUT4 mRNAs did not differ between $Skp2^{+/+}$ MEFs and $Skp2^{+/-}$ MEFs at 10 days after the onset of differentiation induction (data not shown). We did not detect an increase in the number of $Skp2^{+/+}$, $Skp2^{+/-}$, or $Skp2^{-/-}$ MEFs even at 60 h after the onset of exposure to inducers of differentiation (Fig. 2C), consistent with the recent finding that neither cell number nor DNA synthesis increased at early time points during adipocyte differentiation in MEFs [24]. In addition, ~76% of $Skp2^{+/+}$ MEFs remained in G_0–G_1 phase of the cell cycle at 18 h (Fig. 2D) or 42 h (data not shown) after the onset of adipogenic induction. These results suggest that Skp2 may play a direct role in adipocyte differentiation in a manner independent of cell division.

Promotion of adipogenesis in MEFs by genetic ablation of $p27^{Kip1}$

To confirm the role of $p27^{Kip1}$ in adipocyte differentiation, we isolated MEFs from $p27^{+/+}$ and $p27^{-/-}$ littermates at embryonic day

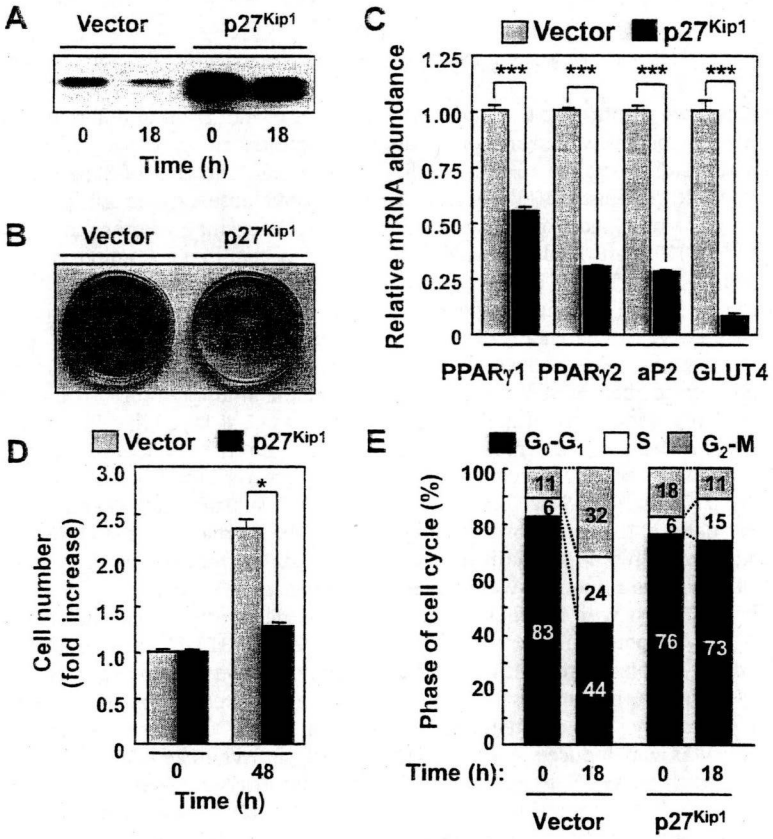

Fig. 1. Effect of forced expression of $p27^{Kip1}$ on adipocyte differentiation in 3T3-L1 cells. (A) 3T3-L1 cells stably expressing $p27^{Kip1}$ or those infected with the corresponding empty vector were subjected to immunoblot analysis with antibodies to $p27^{Kip1}$ at the indicated times after exposure to MDI. (B, C) 3T3-L1 cells overexpressing $p27^{Kip1}$ or those infected with the empty vector were stained with oil red O (B) or subjected to qRT-PCR analysis of PPARγ1, PPARγ2, 442/aP2, and GLUT4 mRNAs (C) at 8 days after the onset of exposure to MDI. Quantitative data are means ± SEM from three separate experiments and are expressed relative to the corresponding value for cells infected with the empty vector. $^{***}P < 0.005$. (D) Number of 3T3-L1 cells overexpressing $p27^{Kip1}$ or those infected with the empty vector after induction of differentiation for 48 h with MDI. Data are expressed relative to the cell number before exposure to MDI and are means ± SEM from three separate experiments. $^{*}P < 0.05$. (E) Number of 3T3-L1 cells overexpressing $p27^{Kip1}$ or those infected with the empty vector were incubated with MDI for 0 or 18 h and then analyzed for phase of the cell cycle by flow cytometry. Data are means of values from three separate experiments.

13.5. Immunoblot analysis verified that $p27^{Kip1}$ was not expressed in MEFs isolated from *p27*$^{-/-}$ mice (Fig. S3). Whereas 30–40% of *p27*$^{+/+}$ MEFs exhibited cytoplasmic lipid accumulation at 10 days after the onset of exposure to inducers of differentiation, 50–60% of *p27*$^{-/-}$ MEFs did so (Fig. 3A). Moreover, the abundance of mRNAs for PPARγ1, PPARγ2, 442/aP2, and GLUT4 was significantly greater in *p27*$^{-/-}$ MEFs than in *p27*$^{+/+}$ cells at this same time point (Fig. 3B).

Effect of depletion of $p27^{Kip1}$ on adipocyte differentiation in Skp2$^{-/-}$ MEFs

We next examined whether depletion of $p27^{Kip1}$ might restore adipogenesis in *Skp2*$^{-/-}$ MEFs. For these experiments, we infected MEFs with an adenoviral vector encoding an siRNA specific for $p27^{Kip1}$ mRNA (p27siRNA) [16,25]. Infection of *Skp2*$^{-/-}$ MEFs with the adenoviral vector encoding p27siRNA, but not that with an adenovirus encoding β-galactosidase, resulted in a marked reduction in the amount of $p27^{Kip1}$ (Fig. 4A) as well as in a pronounced increase in cell number apparent 48 h after removal of the virus under normal growth conditions (data not shown). However, the number of p27siRNA-expressing *Skp2*$^{-/-}$ MEFs did not differ significantly from that of the control *Skp2*$^{-/-}$ MEFs at 60 h after exposure to inducers of differentiation (data not shown). Furthermore, depletion of $p27^{Kip1}$ in *Skp2*$^{-/-}$ MEFs did not restore lipid accumulation (Fig. 4B) or the expression of adipocyte marker genes (Fig. 4C). These findings suggest that the impairment of adipogenesis induced by ablation of *Skp2* in MEFs is independent of the accumulation of $p27^{Kip1}$.

Effect of troglitazone on adipocyte differentiation in Skp2$^{-/-}$ MEFs

We finally examined whether activation of PPARγ might restore adipogenesis in *Skp2*$^{-/-}$ MEFs. For these experiments, we used troglitazone, a thiazolidinedione drug that serves as a high-affinity ligand for PPARγ [26]. Exposure of *Skp2*$^{-/-}$ MEFs to 10 μM troglitazone in the presence of inducers of adipocyte differentiation increased the abundance of PPARγ1 and PPARγ2 mRNAs, especially that of the latter isoform, as well as promoted lipid accumulation (Fig. 4D and E), suggesting that Skp2 controls adipogenesis in MEFs through regulation of PPARγ activation.

Conclusions

We have shown here that Skp2 plays an essential role in the differentiation of MEFs into adipocytes, and that this function of Skp2 is mediated, at least in part, in a manner independent of $p27^{Kip1}$ expression. The identity of the protein (or proteins) regulated by Skp2 during adipocyte differentiation remains to be determined definitively. Given that Skp2 targets not only $p27^{Kip1}$ but also $p21^{Cip1}$, $p57^{Kip2}$, p130, cyclin E, and other substrates [27], it has been unclear to what extent the degradation of regulatory proteins other than $p27^{Kip1}$ by the Skp2-mediated pathway might contribute to adipocyte differentiation. However, we found that troglitazone, a high-affinity ligand of PPARγ, largely restored adipogenesis in *Skp2*$^{-/-}$ MEFs. The downstream effector molecule of Skp2 in the regulation of adipocyte

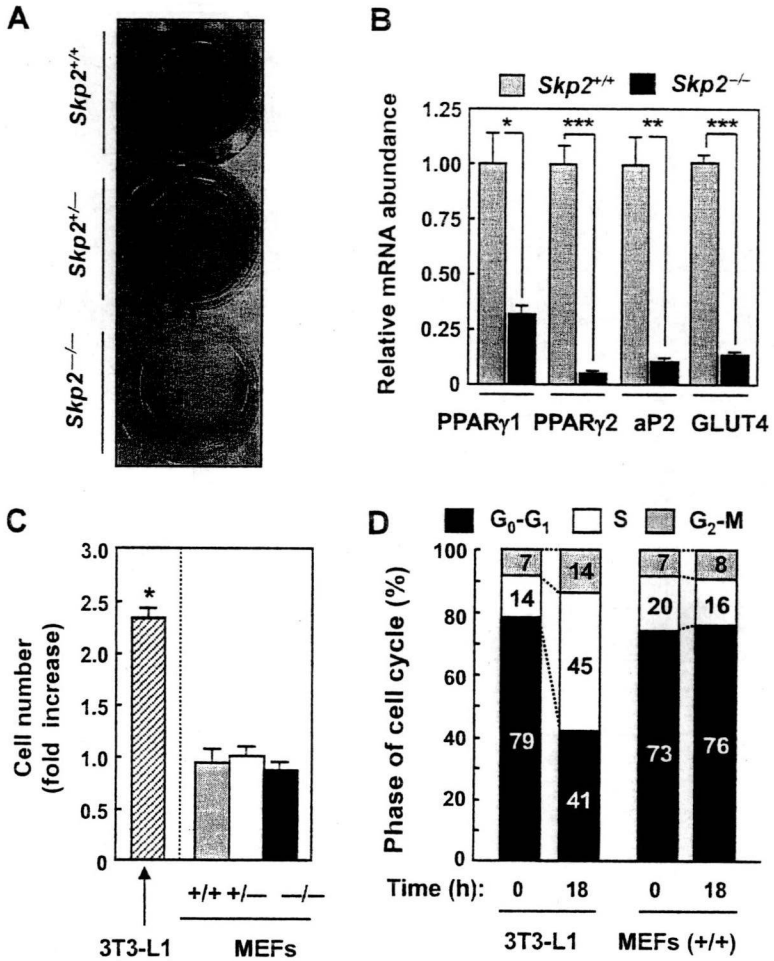

Fig. 2. Effect of *Skp2* ablation on the differentiation of MEFs into adipocytes. (A, B) MEFs of the indicated *Skp2* genotypes were stained with oil red O (A) or subjected to qRT-PCR analysis of PPARγ1, PPARγ2, 442/aP2, and GLUT4 mRNAs (B) at 10 days after the onset of exposure to MDI for induction of adipocyte differentiation. Data in B are expressed relative to the corresponding value for $Skp2^{+/+}$ cells and are means ± SEM from three separate experiments. $^{*}P < 0.05$, $^{**}P < 0.01$, $^{***}P < 0.005$. (C) Number of 3T3-L1 cells or of MEFs of the indicated *Skp2* genotypes at 48 or 60 h, respectively, after the onset of treatment with MDI. Data are expressed relative to the cell number before exposure to MDI and are means ± SEM from three separate experiments. $^{*}P < 0.05$. (D) 3T3-L1 cells or $Skp2^{+/+}$ MEFs were exposed to MDI for 0 or 18 h and then subjected to flow cytometric analysis of phase of the cell cycle. Data are means from three separate experiments.

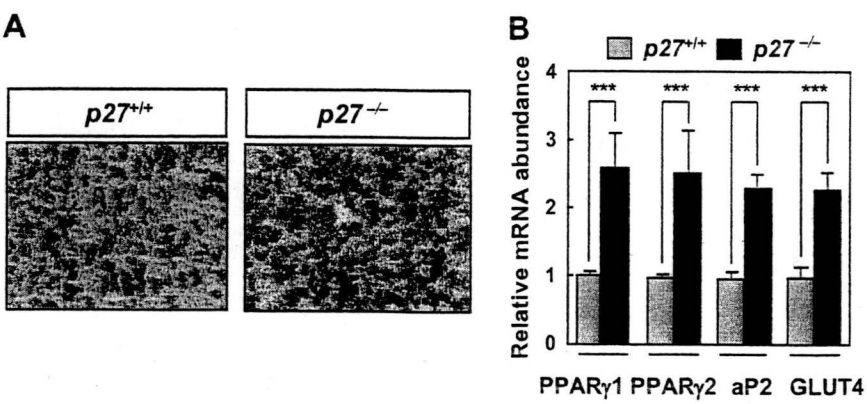

Fig. 3. Effect of genetic ablation of $p27^{Kip1}$ on the differentiation of MEFs into adipocytes. (A, B) MEFs of the indicated *p27* genotypes were stained with oil red O (A) or subjected to qRT-PCR analysis of PPARγ1, PPARγ2, 442/aP2, and GLUT4 mRNAs (B) at 10 days after the onset of exposure to MDI for induction of adipocyte differentiation. Images in B were obtained at a magnification of ×40. Data in B are expressed relative to the corresponding value for $p27^{+/+}$ cells and are means ± SEM of values from three separate experiments. $^{***}P < 0.005$.

differentiation in MEFs may thus be a repressor protein of PPARγ. Cyclin D1 has been shown to inhibit both the expression and transactivation activity of PPARγ [28]. Although Skp2 does not directly target cyclin D1 for degradation, the expression of cyclin D1 is moderately increased in $Skp2^{-/-}$ MEFs [11,29]. Skp2 also directly inhibits the expression of the forkhead transcription factor FoxO1 through ubiquitin-mediated degradation [30]. FoxO1 regulates adipocyte differentiation by functioning as an antiadipogenic

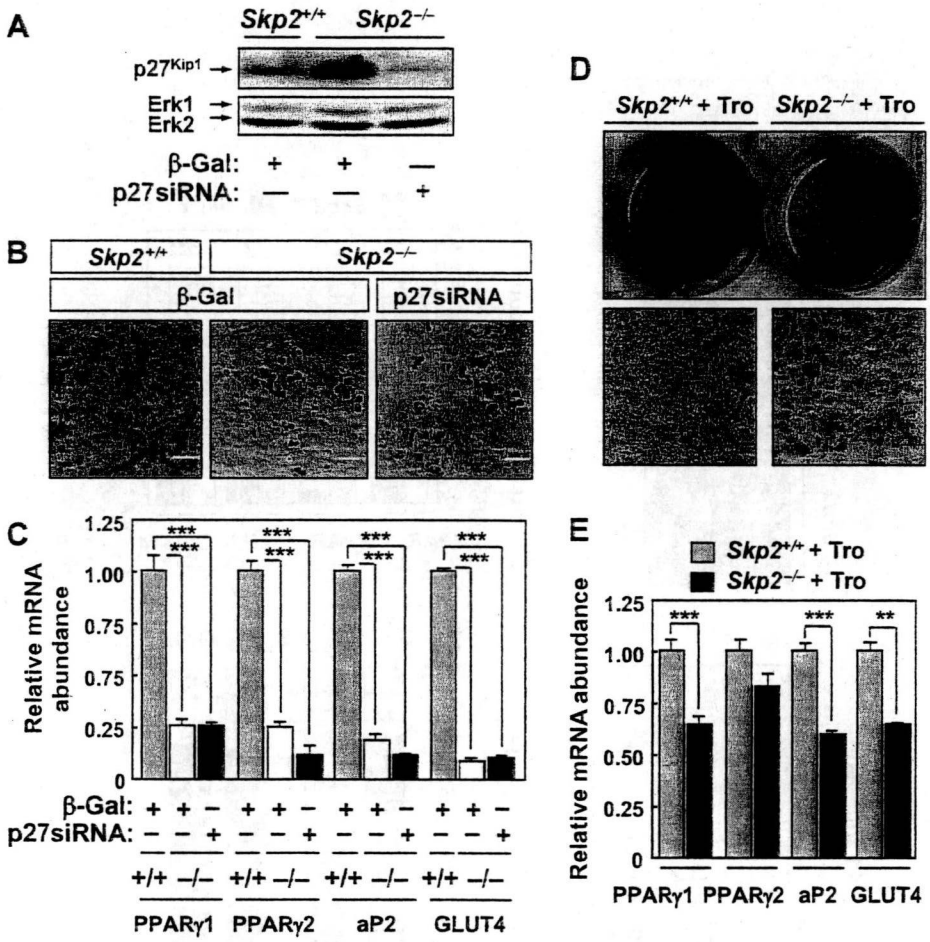

Fig. 4. Effects of $p27^{Kip1}$ depletion and of troglitazone on adipocyte differentiation in $Skp2^{-/-}$ MEFs. (A) Immunoblot analysis of $p27^{Kip1}$ in $Skp2^{+/+}$ MEFs infected with an adenovirus encoding β-galactosidase (β-Gal) or in $Skp2^{-/-}$ MEFs infected with an adenovirus encoding β-galactosidase or p27siRNA. The analysis was performed immediately before exposure of the cells to MDI for induction of adipocyte differentiation. (B, C) $Skp2^{+/+}$ or $Skp2^{-/-}$ MEFs infected as in A were exposed to MDI and either stained with oil red O (B) or subjected to qRT-PCR analysis of PPARγ1, PPARγ2, 442/aP2, and GLUT4 mRNAs (C) after 10 days. Scale bar, 50 μm. Data in C are expressed relative to the corresponding value for $Skp2^{+/+}$ MEFs infected with the adenovirus encoding β-galactosidase and are means ± SEM from three separate experiments. $^{***}P < 0.005$. (D, E) MEFs of the indicated *Skp2* genotypes were exposed to MDI in the presence of 10 μM troglitazone (Tro) and were stained with oil red O (D) or subjected to qRT-PCR analysis of PPARγ1, PPARγ2, 442/aP2, and GLUT4 mRNAs (E) after 10 days. Images in D are macroscopic (upper) and microscopic (lower) views; scale bar, 50 μm. Data in E are expressed relative to the corresponding value for $Skp2^{+/+}$ MEFs and are means ± SEM from three separate experiments. $^{**}P < 0.01$, $^{***}P < 0.005$.

transcription factor [31]. Furthermore, FoxO1 has been shown to inhibit the DNA binding activity of PPARγ [32]. Cyclin D1 and FoxO1 are thus potential targets of Skp2 in the regulation of adipocyte differentiation.

Acknowledgments

We thank K. Nakayama, K. I. Nakayama, and I. Saitho for *Skp2* $^{+/-}$ mice, $p27^{+/-}$ mice, and the adenoviral vector for β-galactosidase, respectively. This work was supported by a grant from Kao Research Council for the Study of Healthcare Science to H.S.; a Grant-in-Aid for Scientific Research on Priority Areas from the Ministry of Education, Culture, Sports, Science, and Technology of Japan (MEXT) to H.S. and M.K.; a grant for the 21st Century COE Program "Center of Excellence for Signal Transduction Disease: Diabetes Mellitus as Model" from MEXT to M.K.; a grant for the Cooperative Link of Unique Science and Technology for Economy Revitalization (CLUSTER) from MEXT to M.K.; Grants-in-Aid for Scientific Research (C) and for Creative Scientific Research from the Japan Society for the Promotion of Science (JSPS) to H.S.; and a Grant-in-Aid for Creative Scientific Research from JSPS to M.K.

Appendix A. Supplementary data

Supplementary data associated with this article can be found, in the online version, at doi:10.1016/j.bbrc.2008.12.069.

References

[1] D.W. Haslam, W.P. James, Obesity, Lancet 366 (2005) 1197–1209.
[2] D.B. Hausman, M. DiGirolama, T.J. Bartness, G.J. Hausman, R.J. Martin, The biology of white adipocyte proliferation, Obesity Rev. 2 (2001) 239–254.
[3] P. Bjorntorp, Size, number and function of adipose tissue cells in human obesity, Horm. Metab. Res. 4 (1974) 77–83.
[4] B.M. Spiegelman, J.S. Flier, Adipogenesis and obesity: rounding out the big picture, Cell 87 (1996) 377–389.
[5] D.O. Morgan, Cyclin-dependent kinases: engines, clocks, and microprocessors, Annu. Rev. Cell Dev. Biol. 13 (1997) 261–291.
[6] C.J. Sherr, J.M. Roberts, CDK inhibitors: positive and negative regulators of G1-phase progression, Genes Dev. 13 (1999) 1501–1512.
[7] K.I. Nakayama, K. Nakayama, Ubiquitin ligases: cell-cycle control and cancer, Nature Rev. Cancer 6 (2006) 369–381.
[8] A. Naaz, D.R. Holsberger, G.A. Iwamoto, A. Nelson, H. Kiyokawa, P.S. Cooke, Loss of cyclin-dependent kinase inhibitors produces adipocyte hyperplasia and obesity, FASEB J. 18 (2004) 1925–1927.
[9] H. Zhang, R. Kobayashi, K. Galaktionov, D. Beach, p19Skp1 and p45Skp2 are essential elements of the cyclin A-CDK2 S phase kinase, Cell 82 (1995) 915–925.

[10] T. Sakai, H. Sakaue, T. Nakamura, M. Okada, Y. Matsuki, E. Watanabe, R. Hiramatsu, K. Nakayama, K.I. Nakayama, M. Kasuga, Skp2 controls adipocyte proliferation during the development of obesity, J. Biol. Chem. 282 (2007) 2038–2046.
[11] K. Nakayama, H. Nagahama, Y.A. Minamishima, M. Matsumoto, I. Nakamichi, K. Kitagawa, M. Shirane, R. Tsunematsu, T. Tsukiyama, N. Ishida, M. Kitagawa, K. Nakayama, S. Hatakeyama, Targeted disruption of Skp2 results in accumulation of cyclin E and p27 (Kip1), polyploidy and centrosome overduplication, EMBO J. 19 (2000) 2069–2081.
[12] K. Nakayama, N. Ishida, M. Shirane, A. Inomata, T. Inoue, N. Shishido, I. Horii, D.Y. Loh, K. Nakayama, Mice lacking p27(Kip1) display increased body size, multiple organ hyperplasia, retinal dysplasia, and pituitary tumors, Cell 85 (1996) 707–720.
[13] T. Mori, H. Sakaue, H. Iguchi, H. Gomi, Y. Okada, Y. Takashima, K. Nakamura, T. Nakamura, T. Yamauchi, N. Kubota, T. Kadowaki, Y. Matsuki, W. Ogawa, R. Hiramatsu, M. Kasuga, Role of Krüppel-like factor 15 (KLF15) in transcriptional regulation of adipogenesis, J. Biol. Chem. 280 (2005) 12867–12875.
[14] H. Sakaue, M. Konishi, W. Ogawa, T. Asaki, T. Mori, M. Yamasaki, M. Takata, H. Ueno, S. Kato, M. Kasuga, N. Itoh, Requirement of fibroblast growth factor 10 in development of white adipose tissue, Genes Dev. 16 (2002) 908–912.
[15] H. Sakaue, W. Ogawa, M. Matsumoto, S. Kuroda, M. Takata, T. Sugimoto, B.M. Spiegelman, M. Kasuga, Posttranscriptional control of adipocyte differentiation through activation of phosphoinositide 3-kinase, J. Biol. Chem. 273 (1998) 28945–28952.
[16] M. Tamamori-Adachi, K. Hayashida, K. Nobori, C. Omizu, K. Yamada, N. Sakamoto, T. Kamura, K. Fukuda, S. Ogawa, K.I. Nakayama, S. Kitajima, Down-regulation of p27Kip1 promotes cell proliferation of rat neonatal cardiomyocytes induced by nuclear expression of cyclin D1 and CDK4. Evidence for impaired Skp2-dependent degradation of p27 in terminal differentiation, J. Biol. Chem. 279 (2004) 50429–50436.
[17] K. Miyake, W. Ogawa, M. Matsumoto, T. Nakamura, H. Sakaue, M. Kasuga, Hyperinsulinemia, glucose intolerance, and dyslipidemia induced by acute inhibition of phosphoinositide 3-kinase signaling in the liver, J. Clin. Invest. 110 (2002) 1483–1491.
[18] H. Green, O. Kehinde, An established preadipose cell line and its differentiation in culture. II. factors affecting the adipose conversion, Cell 5 (1975) 19–27.
[19] S.R. Farmer, Transcriptional control of adipocyte formation, Cell Metab. 4 (2006) 263–273.
[20] Y.M. Patel, M.D. Lane, Mitotic clonal expansion during preadipocyte differentiation: calpain-mediated turnover of p27, J. Biol. Chem. 275 (2000) 17653–17660.
[21] C.A. Auld, R.F. Morrison, Evidence for cytosolic p27(Kip1) ubiquitylation and degradation during adipocyte hyperplasia, Obesity 14 (2006) 2136–2144.
[22] C.A. Auld, C.D. Caccia, R.F. Morrison, Hormonal induction of adipogenesis induces Skp2 expression through PI3K and MAPK pathways, J. Cell. Biochem. 100 (2007) 204–216.
[23] C.A. Auld, R.G. Hopkins, K.M. Fernandes, R.F. Morrison, Novel effect of helenalin on Akt signaling and Skp2 expression in 3T3-L1 preadipocytes, Biochem. Biophys. Res. Commun. 346 (2006) 314–320.
[24] K.A. Kim, J.H. Kim, Y. Wang, H.S. Sul, Preadipocyte factor-1 (Pref-1) activates MEK/ERK pathway to inhibit adipocyte differentiation, Mol. Cell. Biol. 27 (2007) 2294–2308.
[25] K. Nakamura, H. Sakaue, A. Nishizawa, Y. Matsuki, H. Gomi, E. Watanabe, R. Hiramatsua, M. Tamamori-Adachi, S. Kitajima, T. Noda, W. Ogawa, M. Kasuga, PDK1 regulates cell proliferation and cell cycle progression through control of cyclin D1 and p27Kip1 expression, J. Biol. Chem. 283 (2008) 17702–17711.
[26] B.M. Spiegelman, PPAR-gamma: adipogenic regulator and thiazolidinedione receptor, Diabetes 47 (1998) 507–514.
[27] K.I. Nakayama, K. Nakayama, Regulation of the cell cycle by SCF-type ubiquitin ligases, Semin. Cell Dev. Biol. 16 (2005) 323–333.
[28] M. Fu, M. Rao, T. Bouras, C. Wang, K. Wu, X. Zhang, Z. Li, T.P. Yao, R.G. Pestell, Cyclin D1 inhibits peroxisome proliferator-activated receptor gamma-mediated adipogenesis through histone deacetylase recruitment, J. Biol. Chem. 280 (2005) 16934–16941.
[29] A.C. Carrano, E. Eytan, A. Hershko, M. Pagano, SKP2 is required for ubiquitin-mediated degradation of the CDK inhibitor p27, Nat. Cell Biol. 1 (1999) 193–199.
[30] H. Huang, K.M. Regan, F. Wang, D. Wang, D.I. Smith, J.M. van Deursen, D.J. Tindall, Skp2 inhibits FOXO1 in tumor suppression through ubiquitin-mediated degradation, Proc. Natl. Acad. Sci. USA 102 (2005) 1649–1654.
[31] J. Nakae, T. Kitamura, Y. Kitamura, W.H. Biggs III, K.C. Arden, D. Accili, The forkhead transcription factor Foxo1 regulates adipocyte differentiation, Dev. Cell 4 (2003) 119–129.
[32] P. Dowell, T.C. Otto, S. Adi, M.D. Lane, Convergence of peroxisome proliferator-activated receptor gamma and Foxo1 signaling pathways, J. Biol. Chem. 278 (2003) 45485–45491.

Biochemical and Biophysical Research Communications 379 (2009) 98–103

Contents lists available at ScienceDirect

Biochemical and Biophysical Research Communications

journal homepage: www.elsevier.com/locate/ybbrc

The Krüppel-like factor KLF15 inhibits transcription of the adrenomedullin gene in adipocytes

Tomoki Nagare [a], Hiroshi Sakaue [a,b,*], Mototsugu Takashima [a], Kazuhiro Takahashi [c], Hideyuki Gomi [d], Yasushi Matsuki [d], Eijiro Watanabe [d], Ryuji Hiramatsu [d], Wataru Ogawa [a], Masato Kasuga [a,e]

[a] Division of Diabetes, Metabolism, and Endocrinology, Department of Internal Medicine, Kobe University Graduate School of Medicine, Kobe 650-0017, Japan
[b] Department of Pharmacology, Kinki University School of Medicine, 377-2 Onohigashi, Osakasayama 589-8511, Japan
[c] Department of Endocrinology and Applied Medical Science, Tohoku University Graduate School of Medicine, Sendai 980-8575, Japan
[d] Pharmacology Research Laboratories, Dainippon Sumitomo Pharma Co. Ltd., Takarazuka 665-0051, Japan
[e] Research Institute, International Medical Center of Japan, Tokyo 162-8655, Japan

ARTICLE INFO

Article history:
Received 3 December 2008
Available online 16 December 2008

Keywords:
KLF15
Adrenomedullin
ChIP-chip
Microarray
Adipocyte
Transcription

ABSTRACT

KLF15 (Krüppel-like factor 15) plays a key role in adipocyte differentiation and glucose transport in adipocytes through activation of its target genes. We have now identified six target genes regulated directly by KLF15 in 3T3-L1 mouse adipocytes with the use of a combination of microarray-based chromatin immunoprecipitation and gene expression analyses. We confirmed the direct regulation by KLF15 of one of these genes, that for adrenomedullin, with the use of a luciferase reporter assay in 3T3-L1 preadipocytes and adipocytes. Such analysis revealed that the most proximal CACCC element in the promoter of the human adrenomedullin gene (located in the region spanning nucleotides −70 and −29) is required for trans-inhibition by KLF15. Furthermore, chromatin immunoprecipitation showed that KLF15 binds to this region of the human adrenomedullin gene promoter in cultured human adipocytes. These results thus implicate KLF15 in the regulation of adrenomedullin expression in adipose tissue.

Krüppel-like factors (KLFs) are transcriptional regulators that contain the C2H2 zinc-finger motif and play diverse roles in the regulation of cell proliferation, cell differentiation, and development [1,2]. All 17 members of the KLF family identified to date bind to GC-rich sequences including GC boxes and GT boxes (also known as CACCC boxes) [2,3]. Certain KLF proteins have been implicated in adipocyte function or in the pathogenesis of obesity [4–9]. We have previously shown that KLF15 regulates adipogenesis through induction of the peroxisome proliferator-activated receptor γ (PPARγ) gene [10]. In addition, overexpression of KLF15 induces adipocyte maturation and expression of the insulin-sensitive glucose transporter GLUT4 [11], although the physiological relevance of KLF15 in the development of obesity has remained unclear. We have also previously shown that KLF15 regulates the expression of mitochondrial acetyl-CoA synthase (AceCS2) in skeletal muscle [12] as well as that of phosphoenolpyruvate carboxykinase in hepatocytes [13]. We have now attempted to identify novel targets of KLF15 in mouse 3T3-L1 adipocytes by a combination of chromatin immunoprecipitation with a promoter oligonucleotide microarray (ChIP-chip) and analysis of gene expression with an expression oligonucleotide microarray. Our results indicate that KLF15 inhibits transcription of the adrenomedullin gene in adipocytes.

Materials and methods

Antibodies, reagents, and cells. Goat polyclonal antibodies to KLF15 and normal goat immunoglobulin G (IgG) were obtained from Santa Cruz Biotechnology (Santa Cruz, CA). Insulin, dexamethasone, and isobutylmethylxanthine were from Sigma (St. Louis, MO). Mouse 3T3-L1 cells were obtained from American Type Culture Collection (Manassas, VA). 3T3-L1 preadipocytes were maintained and induced to differentiate into adipocytes as previously described [14]. Cultured human subcutaneous adipocytes (F-SA-75) were obtained from DS Pharma Biomedical (Osaka, Japan).

Adenoviral vectors and infection. An adenoviral vector encoding rat KLF15 (AxKLF15) was generated as previously described [10]. An adenoviral vector encoding β-galactosidase (Axβgal) was kindly provided by I. Saito (University of Tokyo, Tokyo, Japan). An adenoviral vector encoding a short hairpin RNA (shRNA) specific for mouse KLF15 mRNA under the control of the mouse U6 promoter (AxshKLF15) and a vector containing the U6 promoter alone

* Corresponding author. Address: Department of Pharmacology, Kinki University School of Medicine, 377-2 Onohigashi, Osakasayama 589-8511, Japan. Fax: +81 72 366 1820.
E-mail address: hsakaue@med.kindai.ac.jp (H. Sakaue).

0006-291X/$ - see front matter © 2008 Elsevier Inc. All rights reserved.
doi:10.1016/j.bbrc.2008.12.020

(AxU6) were generated described in Supplementary materials and methods. 3T3-L1 preadipocytes or adipocytes were infected with adenoviral vectors as previously described [15].

Expression microarray analysis. Fully differentiated 3T3-L1 adipocytes at 7 days after the onset of induction of differentiation were infected with adenoviral vectors encoding KLF15 or β-galactosidase for 48 h. Total RNA was then isolated from the infected cells with the use of an RNeasy Lipid Tissue Mini Kit (Qiagen, Hilden, Germany). Portions (20 μg) of the RNA were used for the synthesis of biotin-labeled cRNA, which in turn was used to probe Murine Genome U74v2 microarrays (Affymetrix, Santa Clara, CA). The arrays were scanned and analyzed as described previously [10].

Promoter array analysis. Fully differentiated 3T3-L1 adipocytes at 9 days after the onset of differentiation induction were detached from culture dishes by exposure to 0.5% trypsin, washed twice with phosphate-buffered saline, lysed, and subjected to chromatin immunoprecipitation (ChIP) with antibodies to KLF15 or normal goat IgG. The resulting precipitates were then subjected to mouse promoter array analysis with a ChIP-DSL system (version M8K 1.0; Aviva Systems Biology, San Diego, CA). The array was scanned with a GenePix4000B instrument (Molecular Devices, Sunnyvale, CA) and analyzed with Array-Pro Analyzer software (Media Cybernetics, Bethesda, MD).

Quantitative RT-PCR analysis. Total RNA was isolated from 3T3-L1 preadipocytes or adipocytes with the use of an RNeasy Lipid Tissue Mini Kit (Qiagen) and was subjected to reverse transcription (RT). Portions of the resulting cDNA were subjected to quantitative real-time polymerase chain reaction (PCR) analysis in a Sequence Detector (model 7900; Invitrogen (Carlsbad, CA), with the use of specific primers and SYBR Green PCR Master Mix (Perkin-Elmer Life Sciences, Waltham, MA). The relative abundance of mRNAs was calculated with 36B4 mRNA as the invariant control. The PCR primers were described in Supplementary materials and methods.

Expression plasmids, reporter plasmids, and site-directed mutagenesis. A mammalian expression vector for mouse KLF15 (pcDNA3.1/KLF15) was generated as previously described [10]. Mammalian expression vectors either encoding the mouse KLF15 shRNA under the control of the mouse U6 promoter or containing the U6 promoter alone were generated by subcloning the corresponding DNA fragments into pcDNA3.1, from which the cytomegalovirus promoter was subsequently deleted. A luciferase reporter plasmid based on pGL3-basic (Promega, Madison, WI) and containing the human adrenomedullin gene promoter was described previously [16,17]. The human adrenomedullin gene promoter sequence in pGL3-basic was subjected to site-directed mutagenesis with the use of a QuikChange II kit (Stratagene, La Jolla, CA). The resulting plasmids were sequenced to confirm the introduced mutations.

Transient transfection and luciferase reporter assays. 3T3-L1 preadipocytes were cultured in 24-well plates and transfected with the use of the Lipofectamine reagent (Invitrogen). Cells in each well were thus transfected with 0.2 μg of the expression plasmid, 0.1 μg of the reporter plasmid, and 0.1 μg of pSV-β-galactosidase control vector (Promega). 3T3-L1 adipocytes were transfected by electroporation as described previously [18]; the amounts of DNA used for transfection were 2 μg of the expression plasmid, 1 μg of the reporter plasmid, and 1 μg of pSV-β-galactosidase for every three wells of a 24-well plate.

All cells were lysed in 100 μl of "1 Time Passive Lysis Buffer" (Promega) after transfection for 48 h, and portions (20 μl) of the lysates were subjected to assays for firefly luciferase (Promega) and β-galactosidase (Clontech, Palo Alto, CA). Promoter activity was determined as the ratio of luciferase to β-galactosidase activities.

ChIP. ChIP analysis was performed with the use of a ChIP assay kit (Upstate Biotechnology, Lake Placid, NY). In brief, cultured human subcutaneous adipocytes were cross-linked for 30 min with 1% formaldehyde in culture medium, washed with ice-cold phosphate-buffered saline, and lysed and sonicated in SDS lysis buffer [1% SDS, 10 mM EDTA, 50 mM Tris–HCl (pH 8.1)] containing aprotinin (1 μg/ml) and leupeptin (1 μg/ml). Lysates were incubated overnight at 4 °C with antibodies to KLF15 or normal goat IgG, after which protein A–agarose was added and each mixture was incubated for an additional 1 h. The precipitated DNA–protein complexes were washed, eluted from the agarose beads, and reverse cross-linked. DNA was extracted with phenol-chloroform and used as a template for PCR analysis with the primers 5′-GTGGCTGAGGAAAGAAAG-3′(sense) and 5′-AAGAAACCACTGAGTGGC-3′ (antisense). The PCR protocol included an initial incubation at 94 °C for 5 min followed by 35 cycles of 94 °C for 30 s, 52 °C for 30 s, and 72 °C for 30 s. The PCR products were fractionated by electrophoresis on a 2% agarose gel and stained with ethidium bromide.

Results and discussion

Screening for novel KLF15 target genes by combined ChIP-chip and expression microarray analysis in 3T3-L1 adipocytes

To identify novel target genes of KLF15 in 3T3-L1 adipocytes, we first performed ChIP-chip analysis. The precipitates obtained by ChIP with antibodies to KLF15 or with normal goat IgG were thus analyzed with mouse promoter oligonucleotide microarrays containing oligonucleotides corresponding to ~6000 distinct genes. Promoter regions of 132 genes showed a reproducibly significant difference in hybridization signal (Fig. 1A). We next profiled genes whose level of expression changed in association with overexpression of KLF15 in 3T3-L1 adipocytes. Total RNA isolated from 3T3-L1 adipocytes infected with adenoviral vectors encoding either KLF15 or β-galactosidase was thus analyzed with mouse oligonucleotide microarrays, revealing that forced expression of KLF15 was accompanied by an increase in the expression of 337 genes and a decrease in that of 274 genes (Fig. 1A). Integration of the ChIP-chip data with the expression microarray data resulted in the identification of six genes whose promoters bound KLF15 and whose expression was either increased (*Slc16a9*, *Cdk9*, *P4ha2*, and *Klf3*) or decreased (*Aprt* and *Adm*), according to a $\log_2$ ratio of >1.0 or <0.5, respectively, in KLF15-overexpresing 3T3-L1 adipocytes (Fig. 1B). Among these genes directly regulated by KLF15, we further investigated the role of KLF15 in transcription of the adrenomedullin gene (*Adm*).

Effect of KLF15 on transcription of Adm in 3T3-L1 cells

Quantitative RT-PCR analysis confirmed that overexpression of KLF15 in 3T3-L1 adipocytes resulted in down-regulation of adrenomedullin mRNA (Fig. 2A and B). Consistent with previous observations, whereas the amount of KLF15 mRNA was increased during the induction of adipocyte differentiation in 3T3-L1 cells (Fig. 2C) [10], that of adrenomedullin mRNA was decreased (Fig. 2D) [16,19]. Furthermore, we found that overexpression of KLF15 in 3T3-L1 preadipocytes resulted in a significant decrease in the amount of adrenomedullin mRNA (Fig. 2E and F). Conversely, depletion of KLF15 in 3T3-L1 adipocytes by RNA interference resulted in an increase in the abundance of adrenomedullin mRNA (Fig. 2G and H). These findings thus suggested that KLF15 inhibits the transcription of *Adm* in 3T3-L1 adipocytes.

Effect of KLF15 overexpression on the activity of the ADM promoter in 3T3-L1 preadipocytes

To confirm that the KLF15-induced down-regulation of adrenomedullin mRNA was attributable to inhibition of *Adm*

A

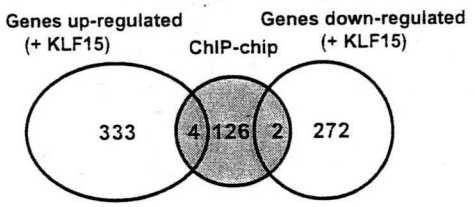

B

Gene symbol	Transcript ID	ChIP-chip	Microarray
Slc16a9	NM_025807	9.6	3.7
Cdk9	NM_130860	8.7	2.3
P4ha2	NM_011031	9.7	2.0
KLF3	NM_008453	7.4	2.0
Aprt	NM_009698	9.6	0.48
Adm	NM_009627	14.8	0.50

Fig. 1. Identification of *Adm* as a target gene of KLF15 in 3T3-L1 adipocytes. (A) Venn diagram of the numbers of genes whose promoters were found to bind KLF15 by ChIP-chip analysis and whose expression was found to be increased or decreased in response to KLF15 overexpression by expression microarray analysis in 3T3-L1 adipocytes. (B) Data for the six genes identified by both types of analysis in (A). The ChIP-chip data are presented as the ratio of the signals obtained for immunoprecipitates prepared with antibodies to KLF15 and with normal goat IgG, whereas the expression microarray data are presented as the ratio of the signals obtained with cells overexpressing KLF15 and those expressing β-galactosidase.

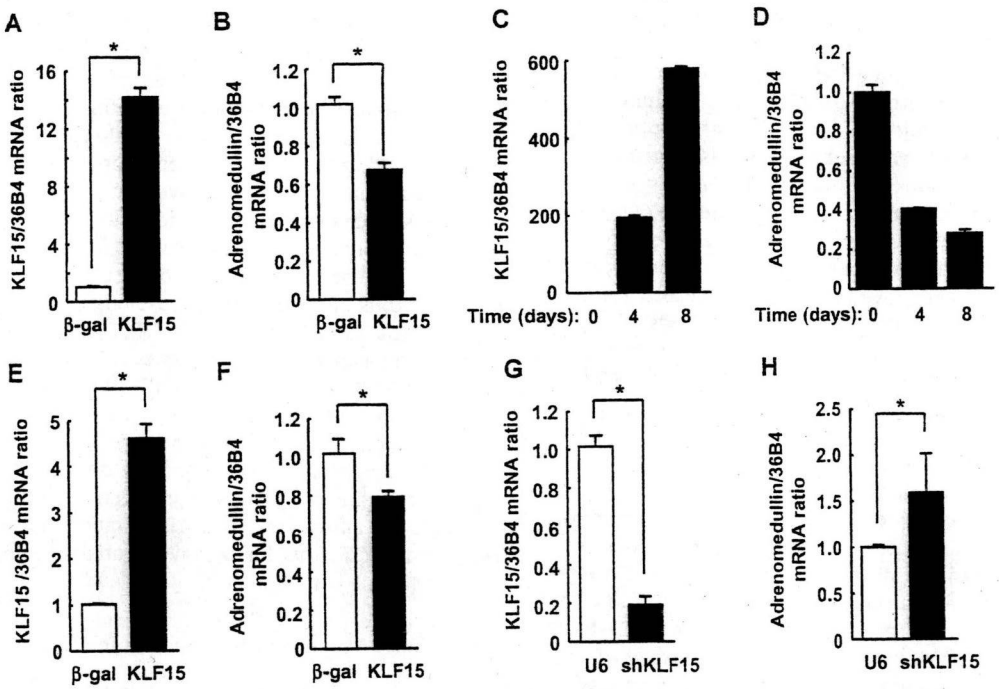

Fig. 2. Effect of KLF15 on transcription of *Adm* in 3T3-L1 cells. (A, B) Effect of overexpression of KLF15 on *Adm* expression in 3T3-L1 adipocytes. 3T3-L1 adipocytes were infected with adenoviral vectors encoding β-galactosidase (β-gal) or rat KLF15 for 48 h, after which the cells were subjected to quantitative RT-PCR analysis of mouse KLF15 (A) and adrenomedullin (B) mRNAs. Data are expressed relative to the corresponding value for cells infected with Axβgal. (C, D) Quantitative RT-PCR analysis of the abundance of KLF15 (C) and adrenomedullin (D) mRNAs at the indicated times after the onset of exposure to inducers of adipocyte differentiation in 3T3-L1 cells. Data are expressed relative to the corresponding value for time zero. (E, F) Quantitative RT-PCR analysis of mouse KLF15 (E) and adrenomedullin (F) mRNAs in 3T3-L1 preadipocytes infected with adenoviral vectors for β-galactosidase or rat KLF15. Data are expressed relative to the corresponding value for cells infected with Axβgal. (G, H) Quantitative RT-PCR analysis of KLF15 (G) and adrenomedullin (H) mRNAs in 3T3-L1 adipocytes infected with adenoviral vectors containing the U6 promoter alone or encoding KLF15 shRNA. Data are expressed relative to the corresponding value for cells infected with the control vector. All RT-PCR data are means ± SEM from three independent experiments. *$P < 0.05$.

transcription, we examined the effect of overexpression of KLF15 in 3T3-L1 preadipocytes on the activity of the human adrenomedullin gene (*ADM*) promoter (nucleotides −4616 to +108 relative to the transcription start site) (Supplementary Fig. 1) ligated to the firefly luciferase gene in the pGL3-basic plasmid. Forced expression of KLF15 resulted in inhibition of *ADM* promoter activity (Fig. 3A). KLF15 was originally identified on the basis of its ability to bind to a GA element in the promoter of the CLC-K1 gene, which encodes a kidney-specific member of the CLC family of Cl^- channels [20]. The gene for GLUT4 in adipose or muscle tissue as well as that for AceCS2 in muscle are also targets of KLF15, which binds to CACCC elements in the promoters of these genes [11,12]. There are 10 CACCC sequences within the 4.6-kb proximal region of the human *ADM* promoter (Supplementary Fig. 1). To determine the relative importance of these sequences as functional KLF15 binding sites, we generated a series of 5′ deletion mutants of the promoter region. Deletion of the sequence from nucleotides −4616 to −71 did not affect transcriptional inhibition by KLF15 (Fig. 3A). However, further deletion to nucleotide −29 resulted in a marked loss of promoter activity as well as rendered such activity insensitive to KLF15 (Fig. 3A). We therefore next constructed two reporter plasmids, pGL3-AM(-70)m1 and pGL3-AM(-70)m2, that contain different mutations of the putative KLF15 binding site located in the region between nucleotides −70 and −29. The promoter activity of the two mutant constructs was unaffected by overexpression of KLF15 (Fig. 3B), indicating that the most proximal putative

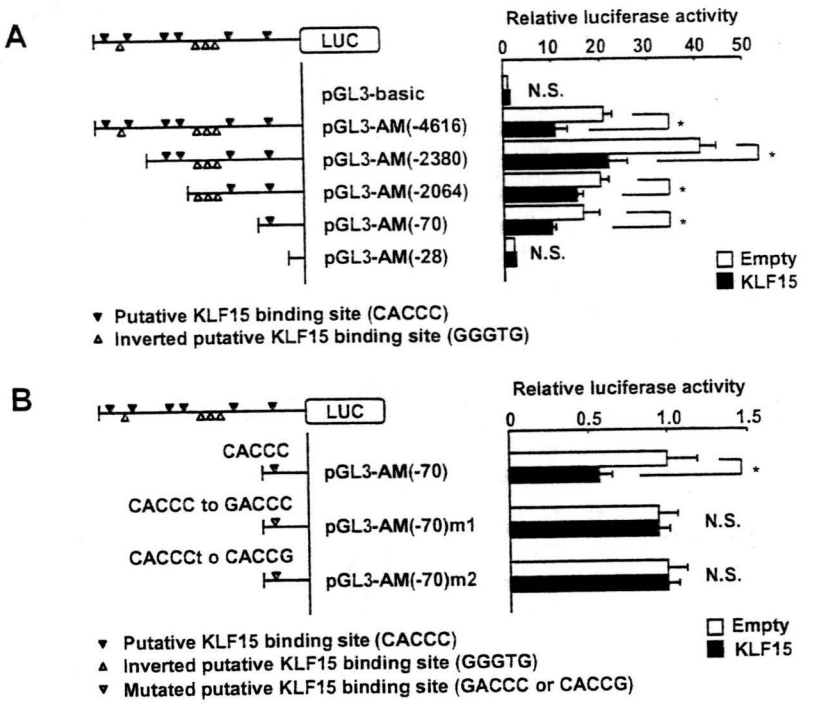

Fig. 3. Effect of KLF15 overexpression on *ADM* promoter activity in 3T3-L1 preadipocytes. 3T3-L1 preadipocytes were transiently transfected with pGL3-basic plasmids containing various deletion (A) or point-mutant (B) constructs of the *ADM* promoter as well as with an expression vector for KLF15 (pcDNA3.1/KLF15) or the corresponding empty vector (pcDNA3.1). Luciferase activity was normalized by β-galactosidase activity derived from pSV-β-galactosidase and is expressed relative to the normalized value for cells transfected with pGL3-basic (A) or pGL3-AM(-70) (B) as well as with the empty expression vector. Data are means ± SEM from three independent experiments. $^{*}P < 0.05$; N.S., not significant.

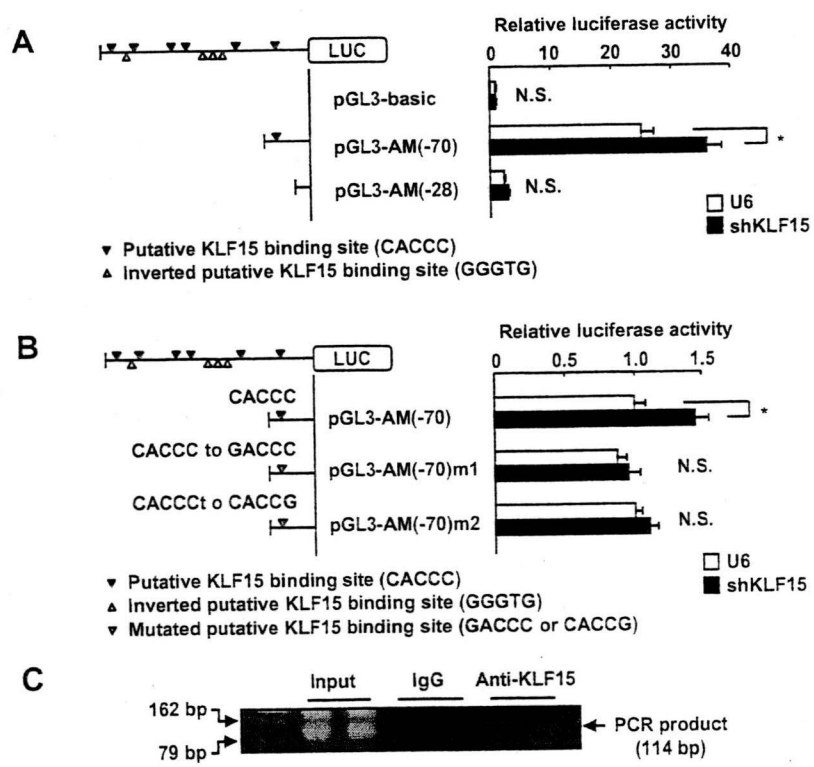

Fig. 4. Effect of depletion of KLF15 on *ADM* promoter activity in 3T3-L1 adipocytes as well as ChIP analysis of KLF15 binding to the *ADM* promoter in human adipocytes. (A, B) 3T3-L1 adipocytes were transiently transfected with the indicated pGL3-basic plasmids as well as with an expression vector for KLF15 shRNA or a control vector containing the U6 promoter alone and were assayed for luciferase activity as in Fig. 3. Data are means ± SEM from three independent experiments. $^{*}P < 0.05$; N.S., not significant. (C) ChIP analysis of the binding of endogenous KLF15 to the *ADM* promoter in cultured human adipocytes (F-SA-75). ChIP was performed with antibodies to KLF15 or with control IgG. The primers used to amplify the *ADM* promoter fragment are indicated in Supplementary Fig. 1.

KLF15 binding site plays the dominant role in trans-inhibition of *ADM* transcription by KLF15.

Effect of depletion of KLF15 on ADM promoter activity in 3T3-L1 adipocytes

Given that depletion of KLF15 induced the expression of *Adm* in 3T3-L1 adipocytes (Fig. 2H), we examined the effect of KLF15 depletion on *ADM* promoter activity in these cells. Transfection of 3T3-L1 adipocytes with a vector encoding KLF15 shRNA resulted in activation of the *ADM* promoter fragment containing the most proximal putative KLF15 binding site in the plasmid pGL3-AM(-70) (Fig. 4A). Furthermore, the m1 or m2 mutations of this putative KLF15 binding site rendered the *ADM* promoter fragment insensitive to KLF15 (Fig. 4B). Finally, a ChIP assay with antibodies to KLF15 showed that KLF15 bound to the region of the *ADM* promoter containing the most proximal putative KLF15 binding site in cultured human adipocytes (Fig. 4C). These results thus indicate that KLF15 binds to the *ADM* promoter and thereby regulates its activity.

Conclusions

We have identified new target genes of KLF15 in 3T3-L1 adipocytes with the combination of ChIP-chip and expression microarray analyses. The proteins encoded by three of these genes – *Slc16a9*, *P4ha2*, and *Aprt* – contribute to transport of monocarboxylic acids [21], collagen biosynthesis [22], and metabolism of purine nucleotides [23], respectively, but they have not been previously characterized in cultured adipocytes or adipose tissue of animals. The protein encoded by *Cdk9* is a member of the cyclin-dependent kinase (CDK) family and has been shown to participate in adipocyte differentiation through direct interaction with and phosphorylation of PPARγ [24]. The protein encoded by *Klf3* also regulates adipogenesis and binds to the promoter of the gene for CCAAT/enhancer-binding protein α (C/EBPα), a key adipogenic gene [5].

Our results suggest that expression of the adrenomedullin gene in cultured adipocytes is suppressed by KLF15 as a result of its interaction with the most proximal CACCC element located in the promoter region spanning nucleotides −70 to −29 of human *ADM*. Deletion of this promoter region resulted in almost a complete loss of transcriptional activity. The transcription factor Sp1 was previously shown to bind to this region of the *ADM* promoter and to induce *ADM* expression during adipocyte differentiation [17,25]. Thus, whereas KLF15 and Sp1 have been shown to induce synergistic activation of the *AceCS2* promoter in vitro [12], these proteins appear to regulate expression of *ADM* in a reciprocal manner.

Adrenomedullin is a potent vasodilatory peptide that was originally isolated from human pheochromocytoma cells [26]. Adipose tissue, especially mature adipocytes, was subsequently shown to be a major source of adrenomedullin in the body, and adipocyte-derived adrenomedullin was found to play a pathophysiologic role in adipogenesis or obesity as a member of the adipokine family of proteins [27,28]. Adipocyte-derived adrenomedullin is also thought to protect against the development of hypertension, insulin resistance, and the complications of these conditions in obese subjects [29]. We have found that expression of *Klf15* is decreased in adipose tissue of mice with high-fat diet–induced or genetic (*ob/ob*) obesity (T.N., H.S., M.K., unpublished observations), animals in which the expression of adrenomedullin in adipose tissue is increased [27]. The role of KLF15 in the regulation of adrenomedullin expression in adipose tissue and its contribution to the pathogenesis of obesity as well as to hypertension, insulin resistance, and their complications associated with obesity thus warrant further investigation.

Acknowledgments

This work was supported by a grant from Takeda Science Foundation to H.S.; a Grant-in-Aid for Scientific Research on Priority Areas from the Ministry of Education, Culture, Sports, Science and Technology of Japan (MEXT) to H.S. and M.K.; a grant for the 21st Century COE Program "Center of Excellence for Signal Transduction Disease: Diabetes Mellitus as Model" from MEXT to M.K.; a grant for the Cooperative Link of Unique Science and Technology for Economy Revitalization (CLUSTER) from MEXT to M.K.; Grants-in-Aid for Scientific Research (C) and for Creative Scientific Research from the Japan Society for the Promotion of Science (JSPS) to H.S.; and a Grant-in-Aid for Creative Scientific Research from JSPS to M.K.

Appendix A. Supplementary data

Supplementary data associated with this article can be found, in the online version, at doi:10.1016/j.bbrc.2008.12.020.

References

[1] D.T. Dang, J. Pevsner, V.W. Yang, The biology of the mammalian Krüppel-like family of transcription factors, Int. J. Biochem. Cell Biol. 32 (2000) 1103–1121.
[2] A.R. Black, J.D. Black, J. Azizkhan-Clifford, Sp1 and krüppel-like factor family of transcription factors in cell growth regulation and cancer, J. Cell. Physiol. 188 (2001) 143–160.
[3] J.J. Bieker, Krüppel-like factors: three fingers in many pies, J. Biol. Chem. 276 (2001) 34355–34358.
[4] S.S. Banerjee, M.W. Feinberg, M. Watanabe, S. Gray, R.L. Haspel, D.J. Denkinger, R. Kawahara, H. Hauner, M.K. Jain, The Krüppel-like factor KLF2 inhibits peroxisome proliferator-activated receptor-gamma expression and adipogenesis, J. Biol. Chem. 278 (2003) 2581–2584.
[5] N. Sue, B.H. Jack, S.A. Eaton, R.C. Pearson, A.P. Funnell, J. Turner, R. Czolij, G. Denyer, S. Bao, J.C. Molero-Navajas, A. Perkins, Y. Fujiwara, S.H. Orkin, K. Bell-Anderson, M. Crossley, Targeted disruption of the basic Krüppel-like factor gene (Klf3) reveals a role in adipogenesis, Mol. Cell. Biol. 28 (2008) 3967–3978.
[6] K. Birsoy, Z. Chen, J. Friedman, Transcriptional regulation of adipogenesis by KLF4, Cell Metab. 4 (2008) 339–347.
[7] Y. Oishi, I. Manabe, K. Tobe, K. Tsushima, T. Shindo, K. Fujiu, G. Nishimura, K. Maemura, T. Yamauchi, N. Kubota, R. Suzuki, T. Kitamura, S. Akira, T. Kadowaki, R. Nagai, Krüppel-like transcription factor KLF5 is a key regulator of adipocyte differentiation, Cell Metab. 1 (2005) 27–39.
[8] D. Li, S. Yea, S. Li, Z. Chen, G. Narla, M. Banck, J. Laborda, S. Tan, J.M. Friedman, S.L. Friedman, M.J. Walsh, Krüppel-like factor-6 promotes preadipocyte differentiation through histone deacetylase 3-dependent repression of DLK1, J. Biol. Chem. 280 (2005) 26941–26952.
[9] Y. Kawamura, Y. Tanaka, R. Kawamori, S. Maeda, Overexpression of Kruppel-like factor 7 regulates adipocytokine gene expressions in human adipocytes and inhibits glucose-induced insulin secretion in pancreatic beta-cell line, Mol. Endocrinol. 20 (2006) 844–856.
[10] T. Mori, H. Sakaue, H. Iguchi, H. Gomi, Y. Okada, Y. Takashima, K. Nakamura, T. Nakamura, T. Yamauchi, N. Kubota, T. Kadowaki, Y. Matsuki, W. Ogawa, R. Hiramatsu, M. Kasuga, Role of Krüppel-like factor 15 (KLF15) in transcriptional regulation of adipogenesis, J. Biol. Chem. 280 (2005) 12867–12875.
[11] S. Gray, M.W. Feinberg, S. Hull, C.T. Kuo, M. Watanabe, S. Sen-Banerjee, A. DePina, R. Haspel, M.K. Jain, The Krüppel-like factor KLF15 regulates the insulin-sensitive glucose transporter GLUT4, J. Biol. Chem. 277 (2002) 34322–34328.
[12] J. Yamamoto, Y. Ikeda, H. Iguchi, T. Fujino, T. Tanaka, H. Asaba, S. Iwasaki, R.X. Ioka, I.W. Kaneko, K. Magoori, S. Takahashi, T. Mori, H. Sakaue, T. Kodama, M. Yanagisawa, T.T. Yamamoto, S. Ito, J. Sakai, A Kruppel-like factor KLF15 contributes to fasting-induced transcriptional activation of mitochondrial acetyl-CoA synthetase gene AceCS2, J. Biol. Chem. 279 (2004) 16954–16962.
[13] K. Teshigawara, W. Ogawa, T. Mori, Y. Matsuki, E. Watanabe, R. Hiramatsu, H. Inoue, K. Miyake, H. Sakaue, M. Kasuga, Role of Krüppel-like factor 15 in PEPCK gene expression in the liver, Biochem. Biophys. Res. Commun. 327 (2005) 920–926.
[14] H. Sakaue, M. Konishi, W. Ogawa, T. Asaki, T. Mori, M. Yamasaki, M. Takata, H. Ueno, S. Kato, M. Kasuga, N. Itoh, Requirement of fibroblast growth factor 10 in development of white adipose tissue, Genes Dev. 16 (2002) 908–912.
[15] H. Sakaue, W. Ogawa, M. Matsumoto, S. Kuroda, M. Takata, T. Sugimoto, B.M. Spiegelman, M. Kasuga, Posttranscriptional control of adipocyte differentiation through activation of phosphoinositide 3-kinase, J. Biol. Chem. 273 (1998) 28945–28952.
[16] Y. Li, Y. Zhang, K. Furuyama, S. Yokoyama, K. Takeda, S. Shibahara, K. Takahashi, Identification of adipocyte differentiation-related regulatory

element for adrenomedullin gene repression (ADRE-AR) in 3T3-L1 cells, Peptides 27 (2006) 1405–1414.
[17] Y. Li, Y. Zhang, S. Shibahara, K. Takahashi, Adrenomedullin in adipocyte differentiation of human mesenchymal stem cells, Biochem. Biophys. Res. Commun. 350 (2006) 616–622.
[18] H. Sakaue, W. Ogawa, T. Nakamura, T. Mori, K. Nakamura, M. Kasuga, Role of MAPK phosphatase-1 (MKP-1) in adipocyte differentiation, J. Biol. Chem. 279 (2004) 39951–39957.
[19] Y. Li, K. Totsune, K. Takeda, K. Furuyama, S. Shibahara, K. Takahashi, Decreased expression of adrenomedullin during adipocyte-differentiation of 3T3-L1 cells, Hypertens. Res. 26 (2003) S41–S44.
[20] S. Uchida, Y. Tanaka, H. Ito, F. Saitoh-Ohara, J. Inazawa, K.K. Yokoyama, S. Sasaki, F. Marumo, Transcriptional regulation of the CLC-K1 promoter by myc-associated zinc finger protein and kidney-enriched Krüppel-like factor, a novel zinc finger repressor, Mol. Cell. Biol. 20 (2000) 7319–7331.
[21] A.P. Halestrap, N.T. Price, The proton-linked monocarboxylate transporter (MCT) family: structure, function and regulation, Biochem. J. 343 (1999) 281–299.
[22] J. Myllyharju, Prolyl 4-hydroxylases, the key enzymes of collagen biosynthesis, Matrix Biol. 22 (2003) 15–24.
[23] F. Delbarre, C. Aucher, B. Amor, A. de Gery, P. Cartier, M. Hamet, Gout with adenine phosphoribosyltransferase deficiency, Biomedicine 21 (1974) 82–85.
[24] I. Iankova, R.K. Petersen, J.S. Annicotte, C. Chavey, J.B. Hansen, I. Kratchmarova, D. Sarruf, M. Benkirane, K. Kristiansen, L. Fajas, Peroxisome proliferator-activated receptor gamma recruits the positive transcription elongation factor b complex to activate transcription and promote adipogenesis, Mol. Endocrinol. 20 (2006) 1494–1505.
[25] Y. Zhang, Y. Li, S. Shibahara, K. Takahashi, Synergistic activation of the human adrenomedullin gene promoter by Sp1 and AP-2alpha, Peptides 29 (2008) 465–472.
[26] K. Kitamura, K. Kangawa, M. Kawamoto, Y. Ichiki, S. Nakamura, H. Matsuo, T. Eto, in: Adrenomedull a novel hypotensive peptide isolated from human pheochromocytoma, Biochem. Biophys. Res. Commun. 192 (1993) 553–560.
[27] R. Harmancey, J.M. Senard, P. Rouet, A. Pathak, F. Smih, Adrenomedullin inhibits adipogenesis under transcriptional control of insulin, Diabetes 56 (2007) 553–563.
[28] T. Nambu, H. Arai, Y. Komatsu, A. Yasoda, K. Moriyama, N. Kanamoto, H. Itoh, K. Nakao, Expression of the adrenomedullin gene in adipose tissue, Regul. Pept. 132 (2005) 17–22.
[29] O. Paulmyer-Lacroix, R. Desbriere, M. Poggi, V. Achard, M.C. Alessi, F. Boudouresque, L. Ouafik, V. Vuaroqueaux, M. Labuhn, A. Dutourand, M. Grino, Expression of adrenomedullin in adipose tissue of lean and obese women, Eur. J. Endocrinol. 155 (2006) 177–185.

Available online at www.sciencedirect.com
ScienceDirect
Metabolism Clinical and Experimental 57 (2008) 373 - 379
Metabolism
Clinical and Experimental
www.elsevier.com/locate/metabol

Short-term effects of dietary fat on intramyocellular lipid in sprinters and endurance runners

Yoshifumi Tamura[a], Hirotaka Watada[a,*], Yasuhiro Igarashi[a], Takashi Nomiyama[a], Tomo Onishi[b], Kouhei Takahashi[b], Susumu Doi[b], Shizuo Katamoto[b], Takahisa Hirose[a], Yasushi Tanaka[a], Ryuzo Kawamori[a]

[a]*Department of Medicine, Metabolism and Endocrinology, Juntendo University School of Medicine, Tokyo 113-8421, Japan*
[b]*Department of Exercise Physiology, Juntendo University School of Health and Sports Science, Chiba, Japan*

Received 10 May 2007; accepted 31 October 2007

Abstract

The effect of short-term fat loading on intramyocellular lipid (IMCL) in different types of muscle in endurance runners and sprinters has not been fully elucidated yet. The purpose of this study was to investigate the effect of dietary lipid on IMCL in soleus muscle (SOL) and tibialis anterior muscle (TA) during training period in endurance runners and sprinters. Seven male endurance runners and 7 male sprinters were selected to participate in the study. We measured TA- and SOL-IMCL levels after 3-day course of isocaloric normal- (25%), high- (60%), and low-fat (10%) diet during training period by ^{1}H–magnetic resonance spectroscopy in each subject. In sprinters, TA- and SOL-IMCL levels were comparable after each diet protocol. However, in endurance runners, TA-IMCL levels after normal-fat and high-fat diets were 1.7 times and 3.0 times higher than that after low-fat diet, respectively. The SOL-IMCL values after normal-fat diet and high-fat diet were 1.5 times and 1.6 times higher than that after low-fat diet, respectively. In addition, the TA-IMCL level after high-fat diet, but not SOL-IMCL, was significantly higher compared with that after normal-fat diet. Our data suggested that short-term dietary fat challenge during training period significantly altered IMCL level in endurance runners, but not in sprinters. In addition, response to fat loading on IMCL was influenced by variation of muscle type in endurance runners. These phenotypic and regional differences might be explained by differences in type of exercise training and muscle fiber composition.

1. Introduction

Recent studies demonstrated that elevated levels of intramyocellular lipid (IMCL), consisting primarily of triglyceride, is associated with insulin resistance [1-4]. High IMCL content is linked to impaired mitochondrial bioenergic and oxidative capacity in skeletal muscle [5-7]. Intramyocellular lipid can be measured noninvasively by proton magnetic resonance spectroscopy (^{1}H-MRS) and is a useful marker of insulin resistance in the clinical setting. However, in endurance-trained athletes, who are profoundly insulin sensitive, IMCL level is paradoxically increased [8]. In addition, IMCL levels correlate with maximal oxygen uptake (Vo_2max) in lean healthy subjects [9]; and exercise training increases IMCL in older adults [10]. Thus, IMCL level is not invariably associated with insulin resistance. Whereas IMCL is well recognized as a physiological marker of skeletal muscle function, IMCL level seems to be affected by various factors that are not yet fully elucidated.

The muscular system consists of various types of muscles that contain different proportions of muscle fiber types. The soleus muscle (SOL) is a typical muscle containing a high proportion of type I muscle fibers (oxidative slow-twitch), whereas the tibialis anterior muscle (TA) is a typical muscle with a large fraction of type II fibers (glycolytic fast-twitch) [11]. It has been reported that sprinters have relatively low type I fiber composition and low aerobic capacity, whereas both of these parameters are high in endurance runners [12]. Previous histochemical studies showed that type I fiber contains 3-fold higher IMCL than type II fiber [13]. Reflecting this difference, the SOL contains ~3-fold greater IMCL than TA [14].

* Corresponding author. Tel.: +81 3 5802 1579; fax: +81 3 3813 5996.
E-mail address: hwatada@med.juntendo.ac.jp (H. Watada).

0026-0495/$ - see front matter © 2008 Elsevier Inc. All rights reserved.
doi:10.1016/j.metabol.2007.10.013

Although the above-mentioned factors are determinants of IMCL, it has been reported also that IMCL is influenced by exercise and dietary fat. Previous studies suggested that endurance exercise decreased IMCL and that high dietary fat is associated with elevated IMCL contents [15-20]. In addition, it has been reported that a high-fat diet (55%-60% fat) for 3 days increased TA-IMCL by ~50%, whereas SOL-IMCL was not significantly affected in healthy subjects. The same study also reported that a low-fat diet (18%-23% fat) did not change IMCL level both in TA and SOL [1]. Similar short-term dietary challenges were applied to endurance runners during training period to enhance their performance because low IMCL may limit exercise performance [21]. However, the effect of fat loading on TA- and SOL-IMCL in endurance runners has not been fully elucidated yet. Accordingly, we hypothesized that a 3-day fat loading may affect IMCL level in endurance runners during training period and that response to fat loading on IMCL might be influenced by variation of muscle type seen in TA and SOL. In addition, the effect of those dietary challenges in sprinters has not been elucidated yet.

The present study was designed to examine the effect of 3-day fat loading on TA- and SOL-IMCL in endurance runners and sprinters during training period. For this purpose, we recruited 7 endurance runners and 7 sprinters. In each subject, we measured TA- and SOL-IMCL levels after a 3-day course of normal-, high-, and low-fat diet. We found that phenotype (endurance runners and sprinters) and muscle type (TA and SOL) influenced changes in IMCL induced by each diet.

2. Methods

2.1. Subjects and preliminary testing

Seven male endurance runners (mean time for running 5000 m = 15 minutes, 32 seconds) and 7 male sprinters (100- to 400-m runners) were selected to participate in the study. All subjects belonged to the track and field club of Juntendo University and were well trained, healthy, and not treated with medications for chronic diseases. All subjects gave written informed consent to the study, which was approved by the Ethics Committee of Juntendo University. The $\dot{V}O_2$max was determined by incremental exercise test with a calibrated mechanically braked cycle ergometer (818E; Monark, Vansbro, Sweden). In this test, the subject began pedaling at 1.5 kiloponds (kp); and the workload was increased by 1 kp every 4 minutes. Subjects were asked to keep a pedaling rate of 50 rpm. After 12 minutes of exercise, the workload was increased by 0.5 kp every 1 minute until exhaustion. Respiratory gas data were averaged every 30 seconds. Respiratory gases were analyzed using open-circuit auto O_2 and CO_2 analyzers with a hot-wire flow meter (AE300S; Minato Medical Science, Osaka, Japan). Total body fat content (% Fat) was measured by a specific analyzer (InBody; BIOSPACE, Tokyo, Japan).

2.2. Study design

The experimental protocol is outlined in Fig. 1. Each subject completed 3 trials in a randomized crossover design, with a 2- to 3-week washout period separating each trial. All subjects consumed low- or high-fat diet after 3 days of control normal-fat diet. The weekly training menu for endurance runners was ~20 km running per day at a self-selected pace (60%-70% of $\dot{V}O_2$max) during the intervention period, whereas that for sprinters was anaerobic running training (30- to 400-m sprint training). Both training menus were almost fixed in each protocol and managed by trainers. In all subjects, a training-free period was scheduled for about 20 hours before the measurement of IMCL. Intramyocellular lipid was measured by ^{1}H-MRS as described below. Afterward, blood samples were obtained from each subject for biochemical tests and respiratory gas analysis.

2.3. Dietary manipulation

During the intervention period, subjects were provided packed meal and prohibited to eat anything else. Every subject was provided isocaloric low-fat (10% fat, 70% carbohydrate, 20% protein), normal-fat (25% fat, 55% carbohydrate, 20% protein), or high-fat diet (60% fat, 20% carbohydrate, 20% protein) followed by 3-day normal-fat diet. The fat composition of high-fat diet was 32% saturated, 40% monounsaturated, and 28% polyunsaturated fatty acid. This fat composition is similar to the common diet of Japanese [22]. The energy and food content–controlled diets were prepared by a food company (Musashino Foods, Saitama, Japan).

2.4. Biochemical tests

Fasting blood glucose and free fatty acid (FFA) were measured using an autoanalyzer (SRL Laboratory, Tokyo, Japan). Plasma insulin and leptin concentrations were determined by radioimmunoassay (LINCO Research, St Charles, MO). Serum adiponectin concentrations were

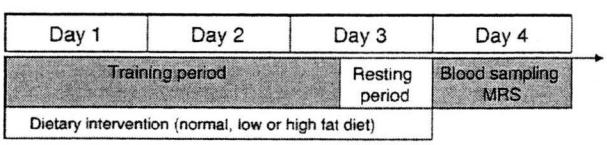

Fig. 1. Experimental protocol. All subjects consumed fat-adjusted foods for 3 days. Weekly training menu for endurance runners was ~20 km running per day at a self-selected pace (60%-70% of $\dot{V}O_2$max) during the intervention period and that for sprinters was anaerobic running training (30- to 400-m sprint training). Both training menus were almost fixed in each protocol and managed by trainers. All subjects had ~20-hour training-free period before the measurement of IMCL. The IMCL values of the right TA and SOL were measured by ^{1}H-MRS.

Table 1
Subjects' characteristics

	Sprinters	Endurance runners
n	7	7
Age (y)	20.7 ± 0.3	21.1 ± 0.4
Height (cm)	174.0 ± 2.2	170.0 ± 1.8 *
Weight (kg)	66.0 ± 2.5	58.4 ± 1.9 *
BMI (kg/m^2)	21.8 ± 0.4	20.2 ± 0.4 *
%Fat	11.5 ± 0.5	12.9 ± 1.0
Vo_2max (mL/[min kg])	49.7 ± 2.7	59.1 ± 6.1 *

Data are mean ± SEM. BMI indicates body mass index.
* $P < .05$ vs sprinters.

measured by an enzyme-linked immunosorbent assay (Otsuka Pharmaceuticals, Tokyo, Japan).

2.5. Proton magnetic resonance spectroscopy

Intramyocellular lipid was measured at fasting state as described previously [23-25]. Briefly, IMCL values of the right TA and SOL were measured by ^{1}H-MRS using a knee coil (VISART EX V4.40; Toshiba, Tokyo, Japan). Voxels (1.2 × 1.2 × 1.2 cm^3) were positioned in the muscle avoiding visible interfascial fat and blood vessels, and the voxel sites were matched carefully at each examination. Imaging parameters were set as follows: repetition time, 1500 milliseconds; echo time, 136 milliseconds; acquisition numbers, 192 and 1024 data points over a 1000-kHz spectral width. After examination, resonances were quantified by reference to the methylene signal intensity (S-fat), with peaks being observed at ~1.25 ppm. Intramyocellular lipid was quantified by the S-fat and using a creatine signal at 3.0 ppm (Cre) as the reference, and was expressed as a ratio relative to Cre (S-fat/Cre).

2.6. Statistical analysis

All data are expressed as mean ± SEM. Differences between 2 groups were tested by unpaired t tests. Repeated-measures analysis of variance and Student-Newman-Keuls test were applied to evaluate the effects of each dietary intervention on IMCL and other measured parameters.

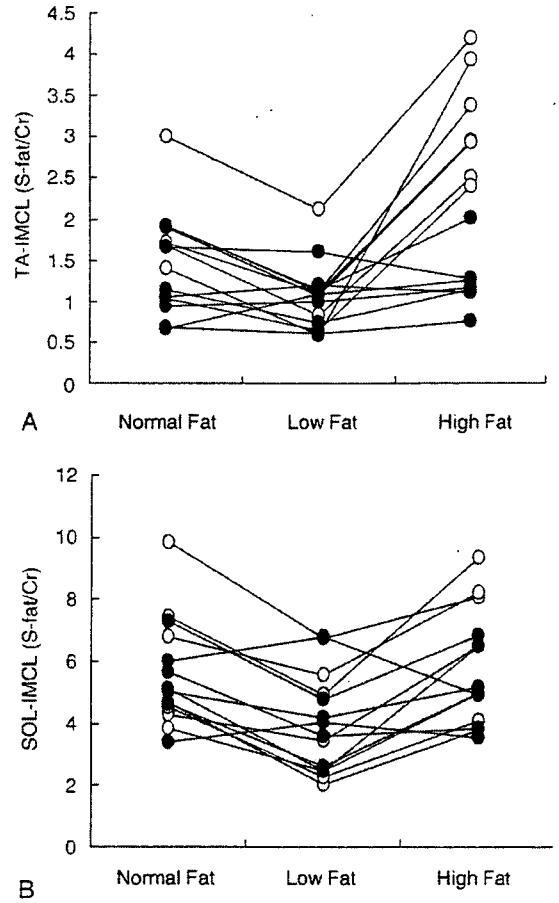

Fig. 2. Individual changes in IMCL values for endurance runners (open circles) and sprinters (closed circles) after dietary intervention in TA (A) and SOL (B). The mean IMCL values are listed in Table 3.

Simple linear regression analysis was performed to evaluate the correlation of metabolic parameters. Statistical significance was set at $P < .05$.

Table 2
Clinical parameters after each dietary intervention for sprinters and endurance runners

	Sprinters			Endurance runners		
	Low fat	Normal fat	High fat	Low fat	Normal fat	High fat
Weight (kg)	66.0 ± 2.4	66.0 ± 2.5	65.6 ± 2.4	58.3 ± 1.8	58.4 ± 1.9	58.0 ± 2.0
%Fat	11.8 ± 0.9	11.5 ± 0.5	11.4 ± 0.8	12.5 ± 1.1	12.9 ± 1.0	12.5 ± 0.9
Insulin (μU/mL)	4.4 ± 0.6	6.2 ± 0.7 *	3.9 ± 0.4 †	4.5 ± 0.4	5.6 ± 0.7	4.6 ± 0.7
Glucose (mg/dL)	90.0 ± 1.3	96.7 ± 1.1 *	87.7 ± 1.9 †	93.1 ± 2.2	93.9 ± 2.0	89.9 ± 2.1
FFA (mmol/L)	0.45 ± 0.03	0.31 ± 0.07	0.56 ± 0.07 †	0.41 ± 0.07	0.35 ± 0.06	0.47 ± 0.08
Leptin (ng/mL)	1.7 ± 0.2	1.3 ± 0.2	1.3 ± 0.2	1.5 ± 0.1	1.5 ± 0.1	1.3 ± 0.1 *
Adiponectin (μg/mL)	6.9 ± 0.4	8.4 ± 0.7 *	6.0 ± 0.5 †	9.7 ± 0.9 ‡	10.8 ± 1.4	8.9 ± 0.9 ‡

Data are mean ± SEM.
† $P < .05$ vs normal fat.
‡ $P < .05$ vs sprinters after same diet protocol.
* $P < .05$ vs low fat.

3. Results

3.1. Characteristics of subjects and high- and low-fat diet–induced changes in metabolic parameters

Table 1 lists the characteristics of participating subjects. The $\dot{V}O_2$max was measured before the study period, and the other data were obtained after the normal-fat–diet period. Endurance runners were significantly shorter, their body mass index was smaller, and $\dot{V}O_2$max was higher than sprinters. Table 2 shows the effects of dietary intervention on various metabolic parameters in the 2 groups of subjects. In both groups, dietary intervention did not change body weight or %Fat. However, fasting blood glucose and insulin concentrations were significantly decreased after low-fat and high-fat diet compared with normal-fat diet protocol in sprinters, but not in endurance runners. In sprinters, serum FFA concentration was significantly higher after high-fat diet than that after normal-fat diet. Serum adiponectin concentrations were significantly lower after low-fat and high-fat diet in sprinters, whereas no such changes were observed in endurance runners. Serum adiponectin concentrations were significantly higher in endurance runners after low-fat and high-fat diet compared with sprinters. Serum leptin concentrations were slightly but significantly decreased in endurance runners after high-fat diet (Table 2).

3.2. Changes in regional IMCL level in sprinters and endurance runners

In sprinters, TA- and SOL-IMCL levels were comparable after each diet protocol. However, in endurance runners, TA-IMCL levels after normal-fat and high-fat diets were 1.7 times and 3.0 times higher than that after low-fat diet, respectively (Fig. 2, Table 3). Furthermore, SOL-IMCL values after normal-fat diet and high-fat diet were 1.5 times and 1.6 times higher than that after low-fat diet, respectively. The TA-IMCL level after high-fat diet, but not SOL-IMCL, was significantly higher compared with that after normal-fat diet. Thus, dietary fat contents significantly altered IMCL level in endurance runners, but not in sprinters. In addition, response to fat loading on IMCL was influenced by variation of muscle type seen in TA and SOL in endurance runners.

The mean TA-IMCL levels of endurance runners after normal- and high-fat diet were significantly higher than those of sprinters, whereas SOL-IMCL was significantly higher only after high-fat diet (Table 3). Especially, the TA-IMCL levels after high-fat diet of all endurance runners were higher than those of sprinters (Fig. 2). On the other hand, TA-IMCL did not correlate with that of SOL after high-fat diet.

3.3. Correlation between IMCL and $\dot{V}O_2$max

In sprinters, TA- and SOL-IMCL levels did not correlate with $\dot{V}O_2$max after each dietary intervention (data not shown). On the other hand, in endurance runners, TA- and SOL-IMCL values after normal-fat and low-fat diet, but not high-fat diet, correlated significantly with $\dot{V}O_2$max (Fig. 3).

4. Discussion

In this study, we found that dietary fat contents influenced IMCL levels, especially TA-IMCL in endurance runners. These changes were only modest in sprinters in both muscle types. The TA-IMCL level after high-fat diet, but not SOL-IMCL, was significantly higher compared with that after normal-fat diet. In addition, TA-IMCL after normal- and low-fat diet correlated significantly with $\dot{V}O_2$max in endurance runners.

Previous reports suggested that endurance exercise reduced IMCL and that the recovery of IMCL was highly dependent on diet composition after exercise [18,19,23]. Larson-Meyer et al [19] demonstrated that 2-hour treadmill run (67% of $\dot{V}O_2$max) decreased SOL-IMCL by ~25%. Moderate-fat diet (35% of energy) allowed IMCL stores to return to baseline by 22 hours and overshoot by 70 hours after exercise [19]. However, low-fat diet (10% of energy) did not result in recovery of IMCL level to baseline level at 70 hours after exercise. Decombaz et al [18] showed that IMCL in TA decreased by 22% to 26% after 2-hour running at 50% $\dot{V}O_2$max. After 30-hour recovery with high-fat diet (55% of energy), the IMCL level was 30% to 45% higher than that pre-exercise, whereas low-fat diet (15% of energy) did not allow IMCL stores to return to baseline. In our protocol, endurance runners did daily training (running ~20 km/d at 60%-70% of $\dot{V}O_2$max); and we evaluated IMCL level after ~20-hour resting after last bout of exercise. In agreement with previous studies, our data suggest that the variation of IMCL level during training period is dependent on the amount of exercise and recovery time as well as dietary fat content in endurance runners.

Table 3
Intramyocellular lipid levels after each dietary intervention for sprinters and endurance runners

	Sprinters			Endurance runners		
	Low fat	Normal fat	High fat	Low fat	Normal fat	High fat
TA-IMCL (S-fat/Cr)	1.05 ± 0.12	1.15 ± 0.18	1.24 ± 0.14	1.07 ± 0.19	1.81 ± 0.23* †	3.18 ± 0.26* † ‡
SOL-IMCL (S-fat/Cr)	4.06 ± 0.55	5.10 ± 0.46	5.30 ± 0.46	3.92 ± 0.70	5.92 ± 0.83 *	6.43 ± 0.83* †

Data are mean ± SEM.

† $P < .05$ vs normal fat.

‡ $P < .05$ vs sprinters after same diet protocol.

* $P < .05$ vs low fat.

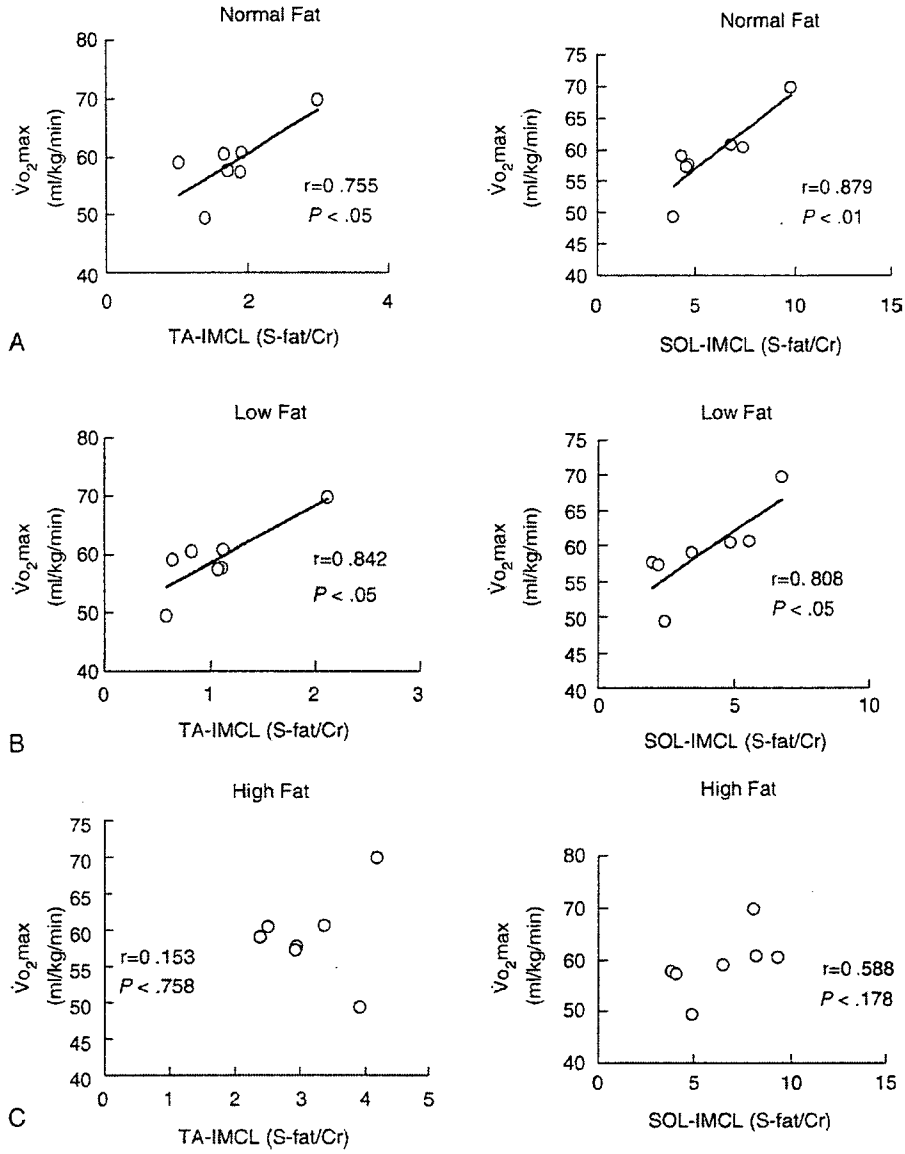

Fig. 3. Relationships between IMCL levels in TA (left) and SOL (right) and $\dot{V}o_2max$ after normal- (A), low- (B), and high-fat (C) dietary intervention in endurance runners.

In the present study, TA-IMCL level after high-fat diet, but not SOL-IMCL, was significantly higher compared with that after normal-fat diet, suggesting that response to fat loading on IMCL during training period was dependent on muscle type in endurance runners. As mentioned above, endurance exercise reduced IMCL and the recovery of IMCL was highly dependent on diet composition after exercise [18,19,23]. From these results, it is speculated that expenditure and recovery of IMCL differ between TA and SOL, thus influencing IMCL level during training period. Consistent with this hypothesis, it has been reported that the increase in TA-IMCL was more pronounced than that in SOL-IMCL after short-term FFA infusion and dietary fat loading, respectively [1]. On the other hand, one bout of prolonged moderate-intensity aerobic exercise reduced TA- and SOL-IMCL; and reduction rates of IMCL seemed to be similar [26,27]. Because SOL contains a high proportion of type I muscle fibers and TA contains a high proportion of type II fibers [11], these regional different response by fat loading might be explained, at least in part, by differences in muscle fiber composition. Further experiments are required to elucidate the exact mechanism of regional difference of IMCL response to exercise and fat loading.

In contrast to these results observed in endurance runners, dietary fat contents did not significantly alter IMCL level in sprinters. Bachmman et al [1] reported that there was high interindividual variation in the increase in IMCL contents by fat loading; and it was suggested that

this variation might reflect insufficient control of parameters, such as physical activity. We also reported previously that 2-week low calorie with low saturated fat diet plus exercise therapy in hospitalized type 2 diabetes mellitus patients resulted in 19% reduction of IMCL and 56% increase in peripheral insulin sensitivity and that these changes were not observed in patients on similar diet restriction but no exercise therapy [23]. In the study, physical activity correlated significantly with the percentage of changes in IMCL and glucose infusion rate [23]. In the present study, the weekly training menu for endurance runners was ~20 km running per day at a self-selected pace (60-70% of $\dot{V}O_2$max) during the intervention period, whereas that for sprinters was anaerobic running training (30- to 400-m sprint training). Thus, it is possible that the different response of IMCL level to dietary fat content between sprinters and endurance runners may be, at least partly, due to the type of exercise training.

In the present study, we observed that TA- and SOL-IMCL after normal-fat and low-fat diet significantly correlated with $\dot{V}O_2$max. In agreement with our data, previous data [8,9] demonstrated that the increase in both IMCL and oxidative capacity is observed in endurance-trained athletes with high $\dot{V}O_2$max and that TA-IMCL levels positively correlate with $\dot{V}O_2$max in lean healthy subjects. In addition, exercise training increases IMCL in older persons in parallel with an enhanced oxidative capacity [10]. Thus, in trained endurance runners, higher IMCL level might reflect enhanced oxidative capacity, which is in part assessed by our measurement of $\dot{V}O_2$max. On the other hand, in this study, IMCL does not correlate with $\dot{V}O_2$max after high-fat diet. It seems that high-fat diet might mask the relationship between IMCL and oxidative capacity. We cannot find the exact reason. Further experiments are required to elucidate the relationship between IMCL and $\dot{V}O_2$max.

Our results showed phenotypic differences in the response of serum adiponectin level to 3-day fat loading. Only in sprinters did serum adiponectin concentrations decrease significantly after low-fat and high-fat diet. Adiponectin is known to increase fat oxidation in muscle and liver, thus improving insulin resistance in rodents [28]. In humans, low adiponectin levels correlated with increased IMCL levels and insulin resistance in muscles [29-31]. Thus, adiponectin might be one of the factors balancing IMCL level after short-term fat change. Further experiments are required to elucidate the relationship between the response of IMCL to fat loading and adiponectin level.

In conclusion, our data suggested that short-term dietary fat challenge during training period significantly altered IMCL level in endurance runners, but not in sprinters. In addition, response to fat loading on IMCL was influenced by variation of muscle type in endurance runners. These phenotypic and regional differences might be explained by differences in type of exercise training and muscle fiber composition.

Acknowledgments

We thank J Makita, M Umeda, and M Hirayama for the ^{1}H-MRS analysis.

This study was supported by Grant-in-Aid for Young Scientists (B) from Japan Society for the Promotion of Science (18700561 to YT) and grant from the Nakatomi Foundation (YT).

References

[1] Bachmann OP, Dahl DB, Brechtel K, Machann J, Haap M, Maier T, et al. Effects of intravenous and dietary lipid challenge on intramyocellular lipid content and the relation with insulin sensitivity in humans. Diabetes 2001;50:2579-84.

[2] Jacob S, Machann J, Rett K, Brechtel K, Volk A, Renn W, et al. Association of increased intramyocellular lipid content with insulin resistance in lean nondiabetic offspring of type 2 diabetic subjects. Diabetes 1999;48:1113-9.

[3] Kelley DE, Goodpaster BH, Storlien L. Muscle triglyceride and insulin resistance. Annu Rev Nutr 2002;22:325-46.

[4] Krssak M, Falk Petersen K, Dresner A, DiPietro L, Vogel SM, Rothman DL, et al. Intramyocellular lipid concentrations are correlated with insulin sensitivity in humans: a 1H NMR spectroscopy study. Diabetologia 1999;42:113-6.

[5] Petersen KF, Befroy D, Dufour S, Dziura J, Ariyan C, Rothman DL, et al. Mitochondrial dysfunction in the elderly: possible role in insulin resistance. Science 2003;300:1140-2.

[6] Kelley DE, He J, Menshikova EV, Ritov VB. Dysfunction of mitochondria in human skeletal muscle in type 2 diabetes. Diabetes 2002;51:2944-50.

[7] He J, Watkins S, Kelley DE. Skeletal muscle lipid content and oxidative enzyme activity in relation to muscle fiber type in type 2 diabetes and obesity. Diabetes 2001;50:817-23.

[8] Goodpaster BH, He J, Watkins S, Kelley DE. Skeletal muscle lipid content and insulin resistance: evidence for a paradox in endurance-trained athletes. J Clin Endocrinol Metab 2001;86:5755-61.

[9] Thamer C, Machann J, Bachmann O, Haap M, Dahl D, Wietek B, et al. Intramyocellular lipids: anthropometric determinants and relationships with maximal aerobic capacity and insulin sensitivity. J Clin Endocrinol Metab 2003;88:1785-91.

[10] Pruchnic R, Katsiaras A, He J, Kelley DE, Winters C, Goodpaster BH. Exercise training increases intramyocellular lipid and oxidative capacity in older adults. Am J Physiol Endocrinol Metab 2004;287:E857-62.

[11] Polgar J, Johnson MA, Weightman D, Appleton D. Data on fibre size in thirty-six human muscles. An autopsy study. J Neurol Sci 1973;19:307-18.

[12] Bergh U, Thorstensson A, Sjodin B, Hulten B, Piehl K, Karlsson J. Maximal oxygen uptake and muscle fiber types in trained and untrained humans. Med Sci Sports 1978;10:151-4.

[13] Essen B, Jansson E, Henriksson J, Taylor AW, Saltin B. Metabolic characteristics of fibre types in human skeletal muscle. Acta Physiol Scand 1975;95:153-65.

[14] Hwang JH, Pan JW, Heydari S, Hetherington HP, Stein DT. Regional differences in intramyocellular lipids in humans observed by in vivo 1H-MR spectroscopic imaging. J Appl Physiol 2001;90:1267-74.

[15] Coyle EF, Jeukendrup AE, Oseto MC, Hodgkinson BJ, Zderic TW. Low-fat diet alters intramuscular substrates and reduces lipolysis and fat oxidation during exercise. Am J Physiol Endocrinol Metab 2001;280:E391-8.

[16] Zderic TW, Davidson CJ, Schenk S, Byerley LO, Coyle EF. High-fat diet elevates resting intramuscular triglyceride concentration and whole body lipolysis during exercise. Am J Physiol Endocrinol Metab 2004;286:E217-25.

[17] van Loon LJ, Koopman R, Stegen JH, Wagenmakers AJ, Keizer HA, Saris WH. Intramyocellular lipids form an important substrate source during moderate intensity exercise in endurance-trained males in a fasted state. J Physiol 2003;553(Pt 2):611-25.

[18] Decombaz J, Schmitt B, Ith M, Decarli B, Diem P, Kreis R, et al. Postexercise fat intake repletes intramyocellular lipids but no faster in trained than in sedentary subjects. Am J Physiol Regul Integr Comp Physiol 2001;281:R760-9.

[19] Larson-Meyer DE, Newcomer BR, Hunter GR. Influence of endurance running and recovery diet on intramyocellular lipid content in women: a 1H NMR study. Am J Physiol Endocrinol Metab 2002; 282:E95-E106.

[20] Zehnder M, Christ ER, Ith M, Acheson KJ, Pouteau E, Kreis R, et al. Intramyocellular lipid stores increase markedly in athletes after 1.5 days lipid supplementation and are utilized during exercise in proportion to their content. Eur J Appl Physiol 2006;98:341-54.

[21] Pendergast DR, Leddy JJ, Venkatraman JT. A perspective on fat intake in athletes. J Am Coll Nutr 2000;19:345-50.

[22] Sasaki S, Takahashi T, Iitoi Y, Iwase Y, Kobayashi M, Ishihara J, et al. Food and nutrient intakes assessed with dietary records for the validation study of a self-administered food frequency questionnaire in JPHC Study Cohort I. J Epidemiol 2003;13(Suppl 1):S23-S50.

[23] Tamura Y, Tanaka Y, Sato F, Choi JB, Watada H, Niwa M, et al. Effects of diet and exercise on muscle and liver intracellular lipid contents and insulin sensitivity in type 2 diabetic patients. J Clin Endocrinol Metab 2005;90:3191-6.

[24] Szczepaniak LS, Babcock EE, Schick F, Dobbins RL, Garg A, Burns DK, et al. Measurement of intracellular triglyceride stores by H spectroscopy: validation in vivo. Am J Physiol 1999;276(5 Pt 1): E977-89.

[25] Ryysy L, Hakkinen AM, Goto T, Vehkavaara S, Westerbacka J, Halavaara J, et al. Hepatic fat content and insulin action on free fatty acids and glucose metabolism rather than insulin absorption are associated with insulin requirements during insulin therapy in type 2 diabetic patients. Diabetes 2000;49:749-58.

[26] Brechtel K, Niess AM, Machann J, Rett K, Schick F, Claussen CD, et al. Utilisation of intramyocellular lipids (IMCLs) during exercise as assessed by proton magnetic resonance spectroscopy (1H-MRS). Horm Metab Res 2001;33:63-6.

[27] Rico-Sanz J, Moosavi M, Thomas EL, McCarthy J, Coutts GA, Saeed N, et al. In vivo evaluation of the effects of continuous exercise on skeletal muscle triglycerides in trained humans. Lipids 2000;35: 1313-8.

[28] Kadowaki T, Yamauchi T. Adiponectin and adiponectin receptors. Endocr Rev 2005;26:439-51.

[29] Perseghin G, Lattuada G, Danna M, Sereni LP, Maffi P, De Cobelli F, et al. Insulin resistance, intramyocellular lipid content, and plasma adiponectin in patients with type 1 diabetes. Am J Physiol Endocrinol Metab 2003;285:E1174-81.

[30] Weiss R, Dufour S, Groszmann A, Petersen K, Dziura J, Taksali SE, et al. Low adiponectin levels in adolescent obesity: a marker of increased intramyocellular lipid accumulation. J Clin Endocrinol Metab 2003;88:2014-8.

[31] Thamer C, Machann J, Tschritter O, Haap M, Wietek B, Dahl D, et al. Relationship between serum adiponectin concentration and intramyocellular lipid stores in humans. Horm Metab Res 2002;34:646-9.